Design of the Control for the Radio Frequency Electron Gun of the VUV-FEL Linac

Daniel Kotthaus

Diplomarbeit
im Fachbereich Physik
der Universität Hamburg

Hamburg
2004

Abstract

At present the VUV-FEL, a free electron laser to generate light in the vacuum ultraviolet part of the spectrum, is built at DESY in Hamburg. The electron source of the VUV-FEL consists of a copper cavity with a resonance frequency of 1.3 GHz. The gradient of the accelerating field is 35 MV/m.

To achieve the quality of the electron beam needed for an FEL, the requirements to the stability of the accelerating field in the electron source are tight. A digital field control system is used to fulfill this requirements. A particular difficulty for the field control is caused by the absence of a pickup antenna to measure the field inside the cavity.

The hardware and the algorithms used for the field control are described in this thesis. Measurements of the achieved field stability and estimations of the expected improvements are presented.

Zusammenfassung

Am DESY in Hamburg wird zurzeit ein Freie Elektronen Laser zur Erzeugung von Laserlicht im vakuum-ultravioletten Teil des Spektrums (VUV-FEL) gebaut. Die Elektronenquelle des VUV-FELs besteht aus einem Kupferresonator, der mit einer Frequenz vom 1.3 GHz betrieben wird. Der Beschleunigungsgradient im Resonator beträgt 35 MV/m.

Um die für Frei Elektronen Laser benötigte Strahlqualität zu erreichen, muss die Stabilität des Beschleunigungsfeldes in der Elektronenquelle hohen Anforderungen genügen. Eine digitale Regelung wird verwendet, um diese Anforderungen zu erfüllen. Eine besondere Schwierigkeit bei der Regelung ist das Fehlen einer Pickup-Antenne mit der das Feld im Resonator direkt gemessen werden kann.

In dieser Arbeit werden die für die Regelung verwendete Hardware und die Algorithmen beschrieben. Messungen der erreichten Feldstabilität und Abschätzungen der noch zu erwartenden Verbesserungen werden vorgestellt.

Contents

Chapter 1

Introduction

In many fields of modern science like material sciences, medicine, biology and chemistry, there is the need for a brilliant source of monochromatic, coherent light in the vacuum ultra violet part of the spectrum[1]. Such requirements can be satisfied by a VUV-FEL[2]. At present the DESY laboratory in Hamburg is building such a light source. This FEL consists of a superconducting linear accelerator for electrons and an undulator[3].

During the construction phase of the VUV-FEL it is also used to investigate the technical requirements for the European X-FEL project, a 3.3 km long linear accelerator with an X-ray FEL planned to be build from 2006 to 2012 [6].

At the VUV-FEL we want to use the SASE effect[4] to generate the coherent light. In a SASE-FEL bunches of electrons are accelerated and sent through an undulator. There the electrons emit light and interact with the light emitted by other electrons within the same bunch. This causes substructures of the bunches, the so called micro-bunches form. The light emitted by the electrons after the formation of the micro-bunches is coherent. This process is explained in detail in [12]. (An FEL could be build without the utilisation of the SASE effect by using an external laser to excite the formation of the microbunches. This is not done at the VUV-FEL.) For the formation of micro-bunches the electron density inside the bunches must very high, the bunches have to be focussed very well. This can only be achieved if the accelerating field in all parts of the accelerator is controlled very precisely. If the beam is defocused too much in the electron source it is impossible to focus it later. Also the arrival time of the electrons and their energy distribution is important for the VUV-FEL. For that reason a good control of the field in the gun is crucial for the whole accelerator.

[1] Vakuum ultra violet (VUV) light has a wavelength of below 100 nm.

[2] VUV-FEL – Vacuum Ultra Violet - Free Electron Laser

[3] An undulator is an alignment of magnets in which the electrons are forced on a sinusoidal track, where they emit light

[4] SASE – Self Amplified Spontaneous Emission

The subject of this thesis is the design of a digital field control for the electron gun of the VUV-FEL.

The next chapter describes the accelerator in general and the different components of the electron gun. The following two chapters give an introduction to the mathematical description of microwave resonators used in the gun and the needed background in control theory. Chapter 5 deals with the setup of the control system. This includes the used hardware as well as the algorithms. The field stability achieved with this setup is presented in chapter 6. The last chapter contains a conclusion and some ideas about possible improvements that could be made in the future.

Chapter 2

Structure of the Accelerator

2.1 The VUV-FEL

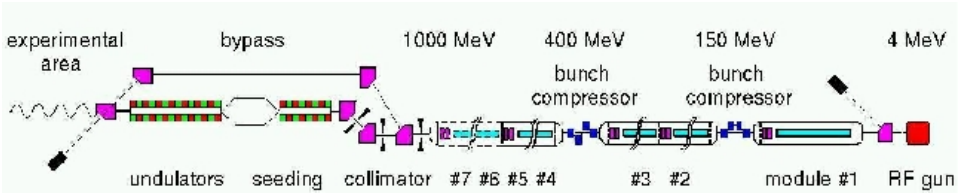

Figure 2.1: Layout of the VUV-FEL

The VUV-FEL linear accelerator is the second stage of the TTF linear accelerator at DESY, Hamburg. It is designed to accelerate electrons to an energy of up to 1 GeV. With the accelerated electrons a free electron laser (FEL) will produce coherent, monochromatic light. The wavelength of the light depends on the energy of the accelerated electrons. It can be tuned by the operators of the accelerator between 6.4 nm and 120 nm. A schematic of the accelerator is shown in figure 2.1.

The source of the electrons is a radio frequency electron gun. This gun will be described in the next section (2.2). The electrons leave the gun in bunches with an energy of 6 MeV per electron. Then they are accelerated by the first acceleration module. An acceleration module of the VUV-FEL linear accelerator consists of a cryostat with eight superconducting nine-cell cavities in the TESLA design (see [5] for a description of these cavities). The acceleration is done by an electromagnetic field of standing waves with a frequency of 1.3 GHz. The field is generated by a klystron which excites the cavities in the π-mode (i.e., the field in one cell of the cavity is shifted by 180° in phase relative to that in the next cell). One nine-cell resonator is

1.04 m long[1], the gradient of the accelerating field is 12 MV/m to 25 MV/m. The first four cavities of the first module are operated at a gradient of 12 MV/m. The energy gain of the electrons in one module of the VUV-FEL accelerator is between 100 MeV and 200 MeV depending on the gradient.

After the first acceleration module comes the first bunch compressor. The bunch compressor is a dispersive magnetic chicane. The length of the trajectory of the electrons in the chicane depends on their energy. The lower the energy, the longer is the way. By inserting the bunch into the first module at a time when the field is rising, the electrons at the end of the pulse receive more energy than those at the front and thus travel a shorter way. When the electrons leave the bunch compressor the bunch is shorter than before. In the two bunch compressors of the VUV-FEL the bunches are compressed from an rms length of 2.2 mm after leaving the gun to $\sigma = 50\,\mu$m at the end of the accelerator (see [15]).

After the electrons left the first bunch compressor they pass through the next two accelerator modules, then the second bunch compressor and then again two accelerating modules. In the future a sixth and probably a seventh accelerating module will be added.

Behind this there is a magnet that can bend the electron beam into a bypass or let it pass through a collimator into the undulators. In the undulators monochromatic, coherent, and polarised light in the vacuum ultra violet (VUV) part of the spectrum is generated by the SASE-FEL process - an interaction of the electrons with the synchrotron light they emit while passing through the undulators. (For a description of the SASE - FEL process see [12].)

After the electrons passed the undulators respectively the bypass they are deflected into a beam dump.

Different diagnostic tools to measure the length and arrival time, the charge and the longitudinal and transversal charge distribution of the bunch, are placed at many locations between the modules. These devices are described in [11].

A part of the energy of the accelerating field is dissipated in the surface of the cavities and heats them. The dissipated power in the cavity is about 10 kW at a gradient of 25 MV/m. To maintain the superconducting state the cavities have to be kept at a temperature of 2 K. The energy needed to supply the refrigerating plant keeping the temperatures at 2 K is about 1000 times higher than the thermal energy that is deposited in the cavity. To compensate the 10 kW dissipated power a refrigerating plant would need 10 MW input power. The energy dissipated in the surface of the normal conducting gun cavity is 3 MW while the field is kept at high gradient.

[1]The length can be calculated as follows: The resonator has 9 cells, each half a wavelength of the resonance frequency long. The resonance frequency is f=1.3 GHz. This gives a length of $l = \frac{9}{2}\frac{c}{f}$=1.04 m, where c is the speed of light.

Tremendous amounts of energy would be needed to keep the superconducting and the normal conducting resonators at operating temperature if the field in the cavities has constantly the desired gradient. Non of our cooling systems is capable of that, therefor the accelerator is not operated in continuous wave mode (cw), but in a pulsed mode with pulses of high field energy ('macropulses') separated by times with no microwave power reaching the cavities.

The time during which the field inside the cavities is at a constant high gradient ('flat top') has a duration of 800 μs. During this time the electron bunches are injected into the cavities. It takes 500 μs to create a field with the desired gradient in the superconducting cavities (see 3.3). The time constant in the normal conducting gun is much smaller, so the filling time is only 30 μs. The filling time could even be shorter, but to avoid peaks of high voltage in the coupler the incident power is not switched to its maximum in one instant. The repetition rate of the macropulses can be varied between 1 Hz and 10 Hz. During the first run (from February until June 2004) a repetition rate of the macropulses of 5 Hz was used. In this pulsed mode the maximum field is in the cavities less than 1% of the time, thus reducing the average power dissipated in the cavities by two orders of magnitude.

During the flat top time, electron bunches are generated inside the gun cavity (see section 2.2) at a rate of one bunch per microsecond. Every bunch has a charge of 1 nC to 2 nC. The spacing of 1 μs between the pulses leads to an average beam current during the flat top time of 1 mA to 2 mA.

During the first run of the VUV-FEL not more than 30 bunches per high energy pulse have been used. For that reason the flat top duration in the gun has been kept short. Normally it was 100 μs.

2.2 The Electron Injector

The electron gun of the VUV-FEL is described more closely in the following. A schematic of the gun is given in figure 2.2.

The Resonator

The central part of the gun is a $1\frac{1}{2}$-cell microwave resonator made from copper. The resonator is a standing wave structure with a 180° phase shift between the field in the full cell and that in the half cell. The length of the cells is chosen in a way that the electrons move through them in the same time the microwave needs to change its sign, i.e., in half of the RF period (385 ps). Since the gradient in the cavities is 30 MV/m, the electrons already have a speed of $\beta = 0.975$ after the first half cell. This means the length of the full cell can be chosen as half the rf wavelength, while the half cell is a bit longer than a quarter of the wavelength ($5/16\,\lambda$). The length of both cells add up to 19 cm.

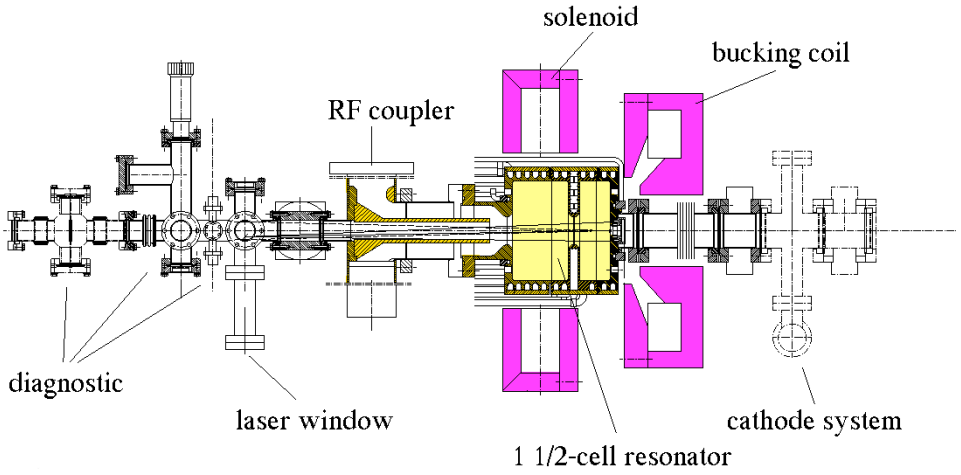

Figure 2.2: Schematics of the electron gun (Picture from [8])

Generation of the Electron Bunches

In the centre of the back side of the half cell is a photo cathode which is coated with Cs_2Te. This cathode is damaged by oxidation when it has contact with the air. Thus it has to stay in ultra high vacuum. A system of valves and and manipulators are installed behind the resonator to render an exchange of the cathode possible while maintaining the vacuum inside the cavity. At the other end of the resonator there is the evacuated beamline through which the electrons leave the gun.

The electron bunches are generated by irradiating the cathode with short pulses from a laser at a wavelength of $\lambda = 262\,\mathrm{nm}$. The photo effect generates free electrons in front of the cathode. With an energy of $1\,\mu\mathrm{J}$ per laser pulse an electron bunch with a charge of 1 nC is produced. These electrons are instantaneously accelerated by the microwave field inside the resonator.

The RF Coupler

The microwave power from a klystron is coupled through the rf input coupler into the cavity, where standing waves form. To avoid the excitation of dipole modes, which would increase the transversal emittance the designers of the gun for the VUV-FEL considered the symmetry very important. To achieve maximum symmetry a coaxial coupler is fitted to the front iris of the whole cell.

Limiting the Beam Emittance

If the electrons are accelerated to relativistic energies a magnetic attraction between them builds up and counteracts the repulsive coulomb force. At very high Lorentz factors γ the sum of the magnetic attraction and the electric repulsion approaches zero. Hence it is crucial to accelerate the electrons as fast as possible to relativistic speed. With an average accelerating field of 30 MV/m the electrons reach a relativistic γ-factor of about $\gamma = 5.2$ after the first half cell and $\gamma = 12$ at the end of the gun.

Around the second cell of the resonator there is a big solenoid magnet. The electrons move parallel to the axis of the solenoid when entering the field of this magnet. An electron that is not on the solenoid axis will cross components of the magnetic flux lines which are directed towards the axis (see figure 2.3). The resulting magnetic force on the electron is tangential

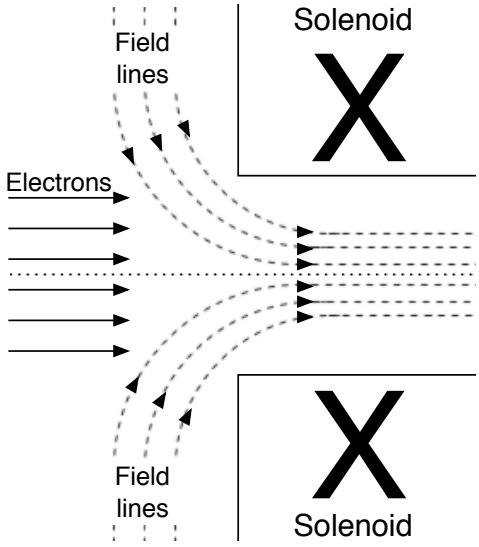

Figure 2.3: Scheme of the magnetic field lines of the solenoid

to a cylinder around the solenoid axis. The effect is that the electron gains a tangential velocity component and starts to move on a helical trajectory around a magnetic field line. For example the electrons in figure 2.3 that enter the field above the axis encounter a Lorentz force directed out of the paper plane.

When the electrons fly further towards the center of the solenoid, they encounter stronger field components parallel to the solenoid axis. The tangential velocity components of the electrons interact with these axial field components and produce a focussing magnetic force on the electrons directed towards the axis of the solenoid. In case of the electrons from the example above the velocity component directed into the paper plane causes a force

on the electrons down towards the axis. For a more detailed description of the solenoid focussing see for example [1].

This focussing force counteracts the space charge effects of the electrons and thus improving the beam emittance.

However, a magnetic field directly at the cathode would deteriorate the emittance. To cancel the magnetic field there, a compensating coil (often called 'bucking coil') is placed behind the cathode (see figure 2.2).

Temperature Control

During the flat top time the microwave will deposit 3 MW of power in the cavity, heating it up. For an 800 μs long flat top at a repetition rate of 10 Hz, the average heating power is 24 kW. A water cooling system is installed around the cavity to remove the thermal energy. Heating the cavity by 1 °C changes the resonance frequency by about 20 kHz. To allow stable operations a feedback system controls the temperature of the gun. The temperature regulation is done by changing the temperature of the cooling water. A closer description of this system is given in [10]. Near the centre of the iris and the cathode the heating of the cavity during flat top time is stronger than in the other parts of the cavity. If the rf power dissipated in the cavity is increased by making longer pulses or increasing the peak power, some parts of the gun body, for example the central iris heat up, because the cooling is not equally effective for all parts of the gun. On the other hand the temperature of the cooling water will decrease in order to remove the additional energy. As long as the gun is kept on resonance the temperature of some points of the gun (e.g. inside the central iris) will rise and and at some points (e.g. at the outer circumference) the temperature will drop on time average if the rf power is increased. There has to be a point where the temperature of the tuned gun is independent of the input power. The temperature sensor used in the temperature control system is located in a hole machined into the iris. By putting it closer to the centre or moving it out, the point where the required temperature does not depend on the input power can be found experimentally. The desired temperature can be set with a precision of ± 0.01°C.

Field Measurements

Compared to many other photo emission guns in use at other accelerators or the older versions used at DESY, the design was more focussed on the cylindrical symmetry. Since a pickup antenna used to measure the field inside the gun might have caused perturbations, no antenna was included in the design of the gun. Any field measurements have to rely on the properties of the incident field and the field reflected at the input coupler. In principle the sum of these two waves has to be the field in the cavity. Another reason

why no pickup antenna was installed inside the gun cavity was that the antenna takes space at the surface of the gun body that is needed for the water cooling system.

To measure the incident and the reflected wave independently a directional coupler is placed at the waveguide near the input coupler of the gun which couples a fraction (-61.2 dB) of the incident wave to one output and an other fraction (-62 dB) of the reflected wave to the other output. Since the cable lengths and the attenuation from the directional coupler to the field detectors is different, they have to be calibrated separately in amplitude and phase. These calibrations have to be precisely matched to get the right result when calculating the field in the cavity.

Another problem is that a directional coupler only has a finite directivity, i.e., there is a crosstalk between the outputs of the directional coupler. In our case the directivity of the forward power in the directional coupler is 46.1 dB, that means -107.3 dB (46.1 dB $= -61.2\,\mathrm{dB} + 107.3\,\mathrm{dB}$) of the reflected power reach the output where only the forward power should be. The directivity of the reflected power is 50.2 dB. This finite directivity can theoretically be compensated by changing the calibration (see chapter 5.2), but this has not yet been accomplished.

Chapter 3

Microwave Resonators

A microwave resonator has many eigenmodes of different frequency. It can be shown that the resonant eigenmodes of the electromagnetic field inside the resonator are orthogonal to each other and form a complete system when combined with the static modes of the field. For that reason the field in a resonator can be expanded into the eigenmodes which can be treated separately. In the case of the accelerator we excite only one eigenmode of the cavity. The considerations in this chapter refer only to one eigenmode.

3.1 Differential Equation for one Eigenmode

Every resonant mode is characterised by its resonance frequency ω_0 and its quality factor Q. The quality factor is defined as 2π times the ratio between the energy W stored in the resonator and the loss of energy per period T of the microwave:

$$Q = \frac{2\pi}{T} \cdot \frac{W}{P_{\text{diss}}} = \omega_0 \frac{W}{P_{\text{diss}}} \tag{3.1}$$

where P_{diss} is the dissipated power and T is the period time of the microwave. Resonators with a single mode at a resonance frequency ω_0 can be described like a harmonic oscillator by a second order linear differential equation:

$$\ddot{V}(t) + a \cdot \dot{V}(t) + \omega_0^2 V(t) = b \cdot \dot{I}(t) \tag{3.2}$$

$\dot{I}(t)$ is an external excitation of the resonator. To describe the coefficients a and b in terms of cavity properties we look at an LCR-circuit (an inductance L, a capacity C and a resistor R are connected in parallel) which is driven by a current from a generator (see figure 3.1). Following Kirchhoff's rules, the current from the generator equals the sum of the currents through the inductance, the capacitor and resistor. With the basic relations between the

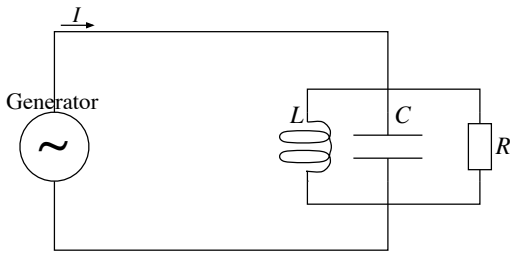

Figure 3.1: The LCR-circuit as a simple equivalent circuit for a cavity

current and the voltage in such components the equation

$$\begin{aligned} I(t) &= \frac{\int V(t)dt}{L} + C\dot{V}(t) + \frac{V(t)}{R} \\ \Rightarrow \frac{\dot{I}(t)}{C} &= \frac{V(t)}{LC} + \ddot{V}(t) + \frac{\dot{V}(t)}{RC} \end{aligned} \tag{3.3}$$

follows (see for example [17]). If the damping term is zero ($\frac{\dot{V}(t)}{RC} = 0$) a solution for the homogeneous part of equation 3.3 is an oscillating voltage $V(t) = V_0 \cos(\omega_0 t)$ with the frequency $f_0 = \frac{\omega_0}{2\pi}$ given by:

$$\omega_0 = \frac{1}{\sqrt{LC}}. \tag{3.4}$$

The power dissipated in the resistance R is

$$P = \frac{V_0^2}{2R} \tag{3.5}$$

and the energy stored in the circuit is

$$W = \frac{CV_0^2}{2} \tag{3.6}$$

The voltage in the LCR-circuit can be identified with the integral of the electric field E_{acc} along the accelerator:

$$V = \int_L E_{\mathrm{acc}}\, \mathrm{d}l \tag{3.7}$$

The result is the accelerating field amplitude. The integration length L is the length where the average accelerating field is of interest, normally the length of one resonator. It follows from the relations 3.4, 3.5, 3.6 and the definition of the quality factor of the resonator (equation 3.1):

$$\begin{aligned} \frac{V_0^2}{2R} &= P = \frac{\omega_0 W}{Q} = \frac{\omega_0 C V_0^2}{2Q} \\ \Rightarrow \frac{1}{RC} &= \frac{\omega_0}{Q} \end{aligned} \tag{3.8}$$

If this is plugged into the differential equation for the LCR-circuit, the result is an equation which contains measurable parameters of the cavity:

$$\ddot{V}(t) + \frac{\omega_0}{Q}\dot{V}(t) + \omega_0^2 V(t) = \frac{\omega_0 R}{Q}\dot{I}(t) \tag{3.9}$$

The resistance R is proportional to the quality factor Q and a factor depending on the geometry of the cavity[1]. It is inversely proportional to the surface resistance of the cavity material.

3.2 Power Transmission to the Cavity

In the LCR-Circuit the power is provided to the fields by a current I from an external generator. In the case of the real cavity the excitation of the field is done by a microwave from a klystron. The microwave is coupled into the cavity through a power coupler which is essentially an antenna. The power from the klystron is used to build up the accelerating field in the cavity. The incident wave is dissipated partly in the walls of the resonator, partly in a load, after it was coupled back out through the input coupler or reflected directly at the coupler[2]. For every way the cavity loses power a different quality factor can be defined according the definition of the quality factor 3.1. If only the power loss P_0 occurring in the cavity walls is taken into account, we speak of the unloaded quality factor Q_0. Looking only at the power P_{ext} lost through the input coupler leads to the external quality factor Q_{ext}. The total power loss without beam is $P_{\text{diss}} = P_{\text{ext}} + P_0$. The effective quality factor of the system consisting of the cavity and the coupler, is called loaded quality factor Q_{L}. Looking at the definition of the quality factor it is obvious that

$$\frac{1}{Q_{\text{L}}} = \frac{1}{Q_0} + \frac{1}{Q_{\text{ext}}} \tag{3.10}$$

If we look at the LCR-circuit model, we can define an effective loaded resistance. The ratio between the power lost through the coupler P_{ext} and the power dissipated in the cavity wall P_0 is called coupling ratio β:

$$\beta := \frac{P_{\text{ext}}}{P_0} = \frac{Q_0}{Q_{\text{ext}}} \tag{3.11}$$

The last two equations give us the relation

$$Q_{\text{L}} = \frac{Q_0}{1+\beta} \tag{3.12}$$

[1] In accelerator physics instead of this resistance often the shunt impedance $R_{\text{sh}} := 2 \cdot R$ is used. The factor two in the relation $P = \frac{V^2}{2R}$, which comes from the time average of the sinusoid voltage, is put into the definition of the resistance. In this thesis I only use the resistance R from the circuit model.

[2] With beam turned on the accelerated electrons also take out power. This will be considered in section 3.4.

For the resistances in the LCR-model we can define an effective loaded resistance by:

$$R_{\mathrm{L}} := \frac{R_0}{1+\beta} \tag{3.13}$$

To protect the klystron from the microwaves reflected from the coupler, there is a circulator between the klystron and the power coupler. This circulator lets the forward power P_{f} from the klystron pass to the coupler. The reflected power P_{r}, including the waves leaking out of the cavity through the coupler, is directed to a load. When viewed from the generator the transmission line is properly matched at the circulator, since there is no reflected power coming back. This leads to the model shown in figure 3.2 with the impedance of the transmission line Z_0 equal to that of the load. The transmission line at the coupler is not necessarily matched to the system

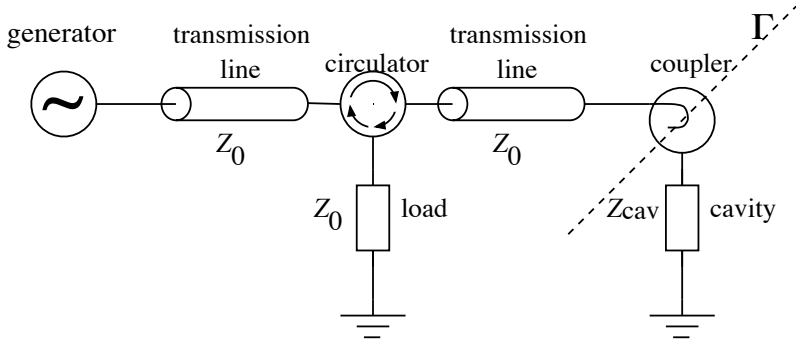

Figure 3.2: Model of the coupling between the klystron and the cavity. A part of the incident wave is reflected at the input coupler. The dashed line marked with Γ is the plane where the incident power is reflected.

of coupler and cavity. If a transmission line is not matched properly, some part of the incident wave is reflected. The ratio between the amplitude of the reflected and the incident wave is called the reflection coefficient Γ. For a transmission line with impedance Z_0 the relation between load impedance Z_{cav} and reflection coefficient is found in many books, e.g.[4]. It is:

$$\Gamma = \frac{Z_{\mathrm{cav}} - Z_0}{Z_{\mathrm{cav}} + Z_0}. \tag{3.14}$$

If the amplitude of the voltage of the electric field at the input coupler is V_0, than the power dissipated in the cavity and the external load is $P_0 = \frac{V_0^2}{2R}$ and $P_{\mathrm{ext}} = \frac{V_0^2}{2Z_0}$. Using the definition of the coupling ratio β (equation 3.11) we get:

$$\begin{aligned} P_{\mathrm{ext}} = \beta \cdot P_0 \quad &\Leftrightarrow \quad \frac{V_0^2}{2Z_0} = \beta \frac{V_0^2}{2R} \\ &\Leftrightarrow \quad R = \beta \cdot Z_0 \end{aligned} \tag{3.15}$$

Plugging this into equation 3.14 gives

$$\Gamma = \frac{\beta - 1}{\beta + 1} \tag{3.16}$$

The voltage of the incident wave V_{for} is either transmitted to the cavity (V_{cav}), or reflected in the opposite direction (V_{ref}). Therefore $V_{\text{cav}} = V_{\text{for}} + V_{\text{ref}}$. Since $V_{\text{ref}} = \Gamma \cdot V_{\text{for}}$ the cavity voltage is:

$$\begin{aligned} V_{\text{cav}} = V_{\text{for}} + V_{\text{ref}} &= (1+\Gamma)V_{\text{for}} \\ &= \Big(1 + \frac{Z_{\text{cav}} - Z_0}{Z_{\text{cav}} + Z_0}\Big)V_{\text{for}} = \frac{2Z_{\text{cav}}}{Z_{\text{cav}} + Z_0}V_{\text{for}} \end{aligned} \tag{3.17}$$

We get the impedance Z_{cav} from the LCR-circuit and with the equations 3.4 and 3.8:

$$Z_{\text{cav}} = \frac{1}{\frac{1}{R} + \frac{1}{i\omega L} + i\omega C} = \frac{R}{1 - i \cdot Q_0\big(\frac{\omega}{\omega_0} - \frac{\omega_0}{\omega}\big)} \tag{3.18}$$

With the definition[3]

$$\tan(\psi) := Q_{\text{L}}\Big(\frac{\omega}{\omega_0} - \frac{\omega_0}{\omega}\Big) \tag{3.19}$$

and equation 3.15 this becomes:

$$Z_{\text{cav}} = \frac{R}{1 - i \cdot \big(\frac{Q_0}{Q_{\text{L}}}\big)\tan(\psi)} = \frac{\beta \cdot Z_0}{1 - i \cdot (\beta + 1)\tan(\psi)} \tag{3.20}$$

Using equation 3.17 we get an expression which tells us what voltage is induced in the cavity, if we have a source with a given voltage and a given frequency:

$$V_{\text{cav}} = \frac{2\beta}{\beta + 1} \cdot \frac{1}{1 - i \cdot \tan(\psi)} V_{\text{for}} \tag{3.21}$$

The average electric field E_{acc} which accelerates the electrons along the cavities can be calculated from the voltage V_{cav} by solving equation 3.7:

$$E_{\text{acc}} = \frac{V_{\text{cav}}}{l_{\text{cav}}} \tag{3.22}$$

where l_{cav} is the length of the cavity. When no electron bunches are in the cavity, in equilibrium the power reaching the cavity equals the dissipated power in the surface resistance. Then the fraction of the power reaching the cavity is:

$$\begin{aligned} \frac{P_{\text{cav}}}{P_{\text{for}}} = \frac{|V_{\text{cav}}|^2}{R} \cdot \frac{Z_0}{|V_{\text{for}}|^2} &= \frac{4\beta}{(\beta+1)^2} \cdot \left|\frac{1}{1 - i \cdot \tan(\psi)}\right|^2 \\ &= \frac{4\beta}{(\beta+1)^2} \cdot \cos^2(\psi) \end{aligned} \tag{3.23}$$

The coupling with $\beta = 1$ is called critical coupling. In this case the amount of power reaching the cavity is maximal for a given forward power.

[3] Why we define this as a tangent will become clear in the next section (3.3)

3.3 Time Constant of the Cavity

With the ansatz $\vec{I}(t) = I_0 e^{i(\omega t)}$ and $\vec{V}(t) = V_0 e^{i(\omega t+\psi)}$ (I_0 and V_0 are complex numbers), we get a stationary solution of equation 3.9:

$$\vec{V}(t) = \frac{RI_0 e^{i(\omega t+\psi)}}{\sqrt{1+\tan^2(\psi)}} \tag{3.24}$$

with $\tan(\psi)$ as in definition 3.19. The angle ψ between the driving current and the excited field is called the tuning angle.

We can now define the detuning as the difference between the resonance frequency f_0 and the frequency f of the driving current $\Delta f := f_0 - f$ or $\Delta\omega := \omega_0 - \omega$. The half bandwidth $f_{1/2}$ is defined as the detuning at which the voltage in the cavity is reduced by a factor of $\frac{1}{\sqrt{2}}$ compared to the voltage achieved with $\Delta f = 0$. If we assume that $\omega_0 \gg \Delta\omega$, equation 3.19 becomes

$$\tan(\psi) = \frac{2Q_L\Delta\omega}{\omega_0}. \tag{3.25}$$

Looking at equation 3.24 we see that $\tan(\psi) = 1$ for $\Delta f = f_{1/2}$. So:

$$\frac{2Q_L 2\pi f_{1/2}}{\omega_0} = 1 \quad \Rightarrow \quad \omega_{1/2} = 2\pi f_{1/2} = \frac{\omega_0}{2Q_L} \tag{3.26}$$

With the assumption that the envelope of the voltage in the cavity V_0 and of the driving current I_0 are changing slowly compared to the harmonic $e^{i\omega t}$ factor of the voltage we can simplify the differential equation of the cavity. If we further assume that we drive the cavity near resonance ($\omega_0 \gg \Delta\omega$) we get a simple linear, first order differential equation for the envelopes of the field and the current as complex numbers V_0 and I_0 with phases relative to a reference with exactly the frequency of the driving power ω:

$$\dot{V}_0(t) = \big(-i(\Delta\omega) - \omega_{1/2}\big)V_0(t) + \omega_{1/2}RI_0(t) \tag{3.27}$$

A mathematical derivation is given in appendix A. A solution for the homogeneous part of the differential equation ($I_0 = 0$) is:

$$V_0(t) = e^{-\omega_{1/2}t} \cdot e^{-i\cdot\Delta\omega t} \tag{3.28}$$

The field decays with a time constant of $\tau = \frac{1}{\omega_{1/2}}$. If the detuning is constant the phase of the field changes linearly with time.

For the cavity of the gun we have a half bandwidth of $f_{1/2} = 59$ kHz and a time constant of $\tau = 2.7$ μs.

3.4 Beamloading

As the electrons are accelerated, they take energy from the field inside the cavity. The current can be added to the driving current in the differential equation for the cavity (equation 3.9). By doing this it has to be taken into account that we only look at the Fourier component of the field that corresponds to the frequency of the excited mode in the resonator. Only the corresponding Fourier component of the beam will interact with this mode of the field. The other components can excite other modes in the resonator, but in the case of the electron gun this is not important. (See ratio of the beam power and the power from the klystron at the end of this section.) It is deduced in [14] for gaussian shaped charge distributions, that the Fourier component I_b is twice that of the direct current I_b0 if the length of the pulses is short compared to the distance between the pulses.

In equilibrium, the field reduction by the beam has to be compensated by the power from the klystron. The following calculations again refer only to the envelopes of the currents and field voltages and their relative angles. Without beam the relation between driving potential and field in the cavity is given by equation 3.21. One can solve this equation for V_cav and add the beam current $I_\mathrm{b} = I_0 e^{i\Theta}$ to it:

$$V_\mathrm{for} = \frac{1+\beta}{2\beta} \cdot \left(1 - i\,\tan(\psi)\right) \cdot V_\mathrm{ref} - Z_0 I_0 e^{i\Theta} \tag{3.29}$$

I use the negative sign, because it is more intuitive if the phase is zero if the acceleration is maximum. The power needed from the klystron is:

$$\begin{aligned} P_\mathrm{for} &= \frac{|V_\mathrm{for}|^2}{2Z_0} \\ &= \frac{(1+\beta)^2 V_\mathrm{cav}^2}{8\beta R}\frac{1}{\cos^2(\psi)} + \frac{I_0^2 R}{8\beta} - \frac{1+\beta}{4\beta\cos(\psi)} V_\mathrm{cav} I_0 \cos(\Theta) \end{aligned} \tag{3.30}$$

With this equation an optimal β can be searched, where the accelerating field for a given power reaching the cavity is at the maximum. It turns out that it is at $\beta = 1 + \frac{P_\mathrm{beam}}{P_\mathrm{cav}}$, with P_beam being the power the beam takes out of the cavity.

The power from the klystron is $P_\mathrm{for} = 3\,\mathrm{MW}$, the amplitude of the accelerating field is $V_\mathrm{cav} = 5.7\,\mathrm{MV}$ (corresponding to a gradient of $30\,\mathrm{MV/m}$ and a resonator length of $0.19\,\mathrm{m}$) and the DC part of the amplitude of the beam current is $I_\mathrm{DC} = 2\,\mathrm{mA}$. The power the beam takes from the cavity field is $P_\mathrm{b} = V_\mathrm{cav} I_\mathrm{b} \cos(\Theta) = 11.4\,\mathrm{kW}$ which is $0.38\,\%$ of the forward power. Thus the beam will only have a small impact on the field in the cavity so the optimal coupling β is in good approximation 1, which is realised in our case.

Note that above given power that is taken from the cavity is the average over long times. The beam needs only 1 ns to leave the cavity. During this

time the power taken out of the cavity is much bigger than on average. The field inside the cavity will drop and refill again until the next bunch enters the cavity.

Chapter 4

Control Theory

As seen in the previous chapter the field in the cavity depends on the detuning $\Delta\omega$. Since the resonance frequency ω_0 is given by the dimensions of the resonator, any mechanical disturbances for example by thermal expansion or vibrations can lead to a disturbance of the accelerating field. Also the output of the klystron changes during the macropulse, even if it is provided with a constant signal at the input. To meet the requirements for the field stability given in 5.1, it is necessary to counteract these fluctuation with a control system. The theoretical background of this control system is given in this chapter.

4.1 Feedback Control

In control theory systems are usually described by the linear state space equations,

$$\dot{\vec{x}}(t) = A\vec{x}(t) + B\vec{u}(t) \tag{4.1}$$

$$\vec{y}(t) = C\vec{x}(t) + D\vec{u}(t) \tag{4.2}$$

where $\vec{x}(t)$ describes the state of the system at the time t and $\vec{u}(t)$ represents the inputs and $\vec{y}(t)$ the outputs (see for example [7]). The system itself is described by the matrices A, B, C and D. The equation for the envelope of the field in the cavity (3.27) is such a state space equation:

$$\dot{V}_0(t) = \big(-i(\Delta\omega) - \omega_{1/2}\big)V_0(t) + \omega_{1/2}RI_0(t)$$

with $A = -i(\Delta\omega) - \omega_{1/2}$ and $B = \omega_{1/2}R$. The second equation (4.2) is used if the outputs of the system are not identical to the state vector $\vec{x}$. The $\vec{y}$ describes the output of the system. The field detectors we use are calibrated to the field amplitude and phase in the wave guide. For that reason we can put $C = 1$. D is zero as long as we do not have any crosstalk directly from the incident wave to the field detectors.

It is convenient to transform the equation 4.1 into the frequency domain by a Laplace transformation:

$$F(s) = \mathcal{L}\big(f(t)\big) = \int_0^\infty e^{-st} f(t)\mathrm{d}t, \tag{4.3}$$

where s is a complex variable. Equation 4.1 transformed this way becomes:

$$\vec{X}s = A\vec{X} + B\vec{U} \tag{4.4}$$

Dividing the outputs of the system $\vec{X}$ by the inputs $\vec{U}$ in the Laplace transformed space gives us the transfer function $H(s)$ of the system. If we assume that the detuning and the bandwidth are constant the transfer function of the cavity is:

$$H_{\mathrm{cav}}(s) = \frac{B}{s - A} = \frac{\omega_{1/2} R}{s + \omega_{1/2} + i\Delta\omega} \tag{4.5}$$

To get the response of the system to an input one has to multiply this input with the transfer function. From this follows that a system composed of n subsystems, where the output of one subsystem is the input of the next subsystem (see figure 4.1) has the transfer function:

$$H(s) = H_{\mathrm{n}}(s) \cdot H_{\mathrm{n\text{-}1}}(s) \cdot \ldots \cdot H_1(s), \tag{4.6}$$

The $H_{\mathrm{i}}(s), i \in [1, n]$ are the transfer functions of the subsystems. A system

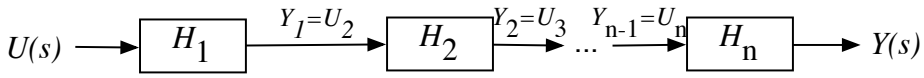

Figure 4.1: Diagram of a system composed of subsystems

with a feedback loop has two subsystems. The output of one subsystem with transfer function $H_1(s)$ is put to the input of the next subsystem ($H_2(s)$). The output of this second system is subtracted from the input to the first subsystem (see figure 4.2). The output of the whole system is:

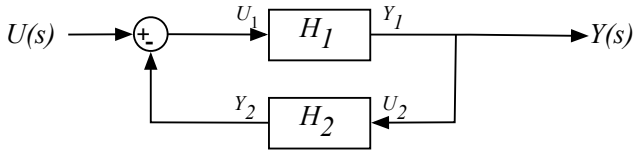

Figure 4.2: Diagram of a system with a feedback loop

$$Y(s) = H_1(s)U_1 = H_1(s)\Big(U - H_2(s)Y(s)\Big) \tag{4.7}$$

From this we get the total transfer function of a system loop[1]:

$$H(s) = H_1(s)\,[1 + H_1(s)H_2(s)]^{-1} \tag{4.8}$$

For the field control of the electron gun we use a digital feedback system. A field detector measures the real and imaginary part of the envelope V_0 of the 1.3 GHz field. The data from the detector is digitised and sent to a digital signal processor (DSP). Every sampling time t_n this processor calculates the deviation of the digitised value V_n from the desired value $\mathrm{SP_n}$. A correction proportional to this deviation and a correction proportional to the integral in time over this error signal are added to the next output of the DSP (PI-control). Since the signal is digitised new values reach the DSP only at discrete times, thus the integral in time becomes a sum. The total output at the time step $t_{\mathrm{n}+1}$ is:

$$\mathrm{Out_n} = \mathrm{FF_n} + G_\mathrm{P}(\mathrm{SP_n} - V_\mathrm{n}) + G_\mathrm{I}\sum_{\mathrm{m}=1}^{\mathrm{n}}(\mathrm{SP_m} - V_\mathrm{m}) \tag{4.9}$$

The time step t_1 is the time where the integrator is turned on. Normally it is at the beginning of the flat top or about 10 μs later. $\mathrm{FF_n}$ is the value of the feedforward (see next section) the DSP would send without feedback. The proportionality factors G_P and G_I are called proportional and integral gain.

Due to the cables, the DSP and the klystron it takes about 4 μs from the measurement of the field until the modified signal reaches the cavity. This is described as a delay in the feedback loop. After we measured the field, we have the possibility to implement a digital lowpass filter. (This filter will be described in section 5.4.6.) Figure 4.3 shows a simplified diagram of the PI-control loop. The transfer function of a proportional gain is just the

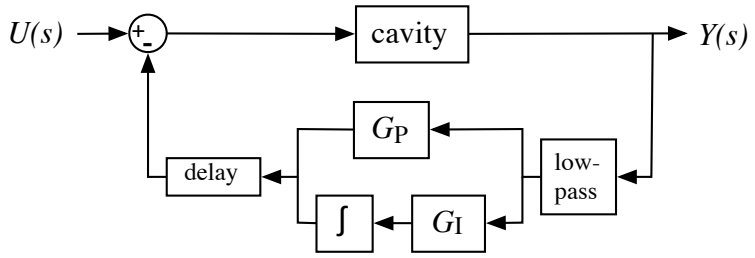

Figure 4.3: Simplified diagram of the PI-control loop

gain factor G_P. An integration becomes a multiplication with $\frac{1}{s}$ after the Laplace transformation. A delay has the transfer function $H_\mathrm{delay} = e^{-T_\mathrm{d}s}$

[1] Of course this works only if the inverse of the matrix $[1 + H_1(s)H_2(s)]$ exists. Since in our case we have normally only complex numbers this is fulfilled.

where T_d is the delay time. The transfer function of a lowpass with the corner frequency ω_c is[2]:

$$H_\mathrm{LP}(s) = \frac{\omega_\mathrm{c}}{s + \omega_\mathrm{c}} \tag{4.10}$$

(The derivation of this functions can be found in [7].) Comparison with equation 4.5 reveals that the cavity acts as a lowpass with corner frequency $\omega_{1/2}$ for the envelope of the field, if the detuning is zero. There are some other components in the control loop, for example the klystron, the vector modulator, the preamplifier, waveguides, and cables. Most of them can be modelled as delays and as lowpasses with corner frequencies which are much higher than that of the cavity. In the following considerations the lowpass character of these additional subsystems is ignored, since the feedback gain has to be near zero for higher frequencies as the following considerations will show. Without the digital filter the total transfer function can be found by using the open loop transfer functions from the last paragraph and the equations 4.6 and 4.8. This gives:

$$H_\mathrm{tot}(s) = \frac{H_\mathrm{cav}}{1 + H_\mathrm{cav}\left(G_\mathrm{P} + \frac{G_\mathrm{I}}{s}\right)e^{-T_\mathrm{d}s}} \tag{4.11}$$

The logarithmic plot of the amplitude and the phase of a transfer function against the frequency $f = \frac{s}{2\pi i}$ is called Bode plot. Figure 4.4 shows the Bode plots of the main parts of the control system of the gun. Mostly due to the delay, the phase change in the control loop increases with the frequency. A phase change of 180° for at a given frequency means the sign of the corresponding Fourier component of the field error changed until the correction is applied. Instead of correcting an error the error will be increased (negative feedback). To avoid this the gain of the control loop has to be well below 1 for frequencies with a phase shift of $\geq 180°$. A gain of 1 should be reached for frequencies corresponding to phase shifts of about 120°. The integrator and the lowpass of the cavity cause a reduction of the gain for higher frequencies (see figure 4.4). To achieve a stable feedback control, we have to limit the proportional gain of the controller to a value that ensures a gain which is low enough for high frequencies, otherwise the system will amplify the Fourier components of disturbances with a frequency corresponding to a phase shift of 180° and oscillations will start.

From the transfer function of a proportional feedback loop with gain G_P ($H = \frac{1}{1+G_\mathrm{P}}$) follows that the error signal is reduced by a factor of $1 + G_\mathrm{P}$.

The gun cavity has a bandwidth of $f_{1/2} = 59\,\mathrm{kHz}$. The delay in our feedback loop is $4\,\mu\mathrm{s}$. Theoretically the maximum gain of the proportional feedback is around $G_\mathrm{P} = 4$. So the error can be reduced to $\frac{1}{1+4} = \frac{1}{5}$.

[2]The corner frequency is the frequency at which the damping of the lowpass is 3 dB

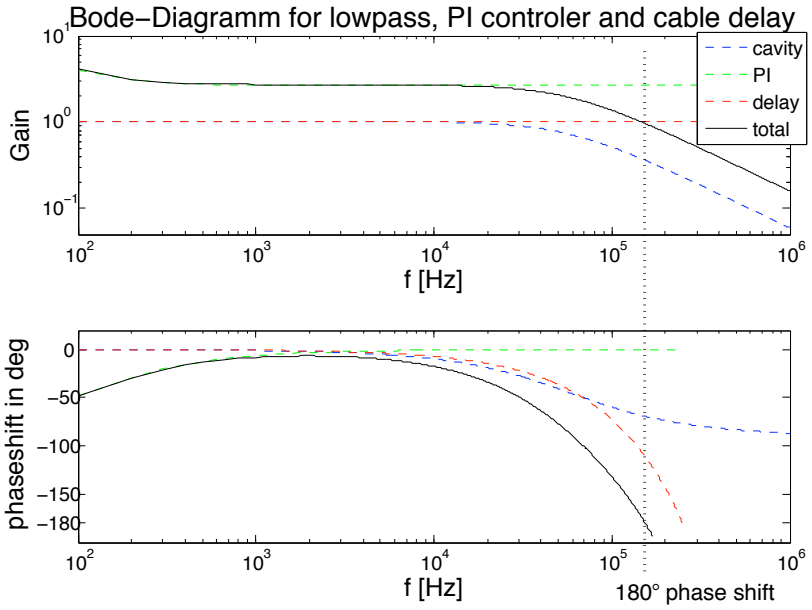

Figure 4.4: Bode plots of some of the parts in the control loop and the resulting closed loop transfer function.

4.2 Feedforward

Since the feedback can reduce errors only to about $\frac{1}{5}$ it is desirable to minimise the errors of the accelerating field before applying the feedback by adapting the incident power. To do this we have a feedforward table. This table has two values for every microsecond of the microwave pulse. These values are proportional to the imaginary and real parts of the wave which is amplified by the preamplifier and the klystron to generate the incident wave.

One pulse of the microwave is usually divided into three parts. The first part is the filling time, where the field inside the resonator is built up. The second part is the flat top. During this time the field inside the cavity should be as stable as possible since the acceleration of the electrons takes place there. The last part is the decay time after the incident power from the klystron is turned off. During this time the detuning and the quality factor of the resonator can be determined quite easily (see section 5.3).

From the equation for the envelope of the field in the cavity (3.27) one can see that the field will follow an exponential curve which approaches a constant value if the driving current and the detuning is constant. The simplest table contains constant values during filling time and flat top and zero everywhere else. A closer inspection of the feedforward is done in chapter 5.4.5.

Currently a feedforward table is used that follows an exponential curve during filling time and is constant during flat top time. It does not take changes of the system parameters into account. If one or more of the parameters change slowly, the table has to be adapted. There are also mechanisms that change the cavity parameters during one microwave pulse in the same way every pulse. In the case of the gun the most important example is the heating of the gun cavity by the dissipated microwave energy in the wall. This leads to an expansion of the resonator and thus to a lower resonance frequency. These repetitive changes lead to repetitive deviations in the accelerating field. To unburden the feedback it is desirable that this errors are corrected by an improved feedforward.

Since we do not exactly know the form of all repetitive errors and the slow drifts of the parameters, we have to use an adaptive feedforward. This means we look at the measured field and calculate a new feedforward table for the next (or a later) pulse. If the field deviates from the desired setpoint at the time t, the correction to the incident wave has to take place at an earlier time. If the transfer function of the cavity is known, it is possible to calculate what correction to the forward power has to be applied to compensate a measured error by inverting the transfer function of the gun and applying this inverted function to the deviation from the setpoint. The transfer function is given in equation 4.5. The inverse is:

$$H_{\mathrm{cav}}^{-1}(s) = \frac{s + \omega_{1/2} + i\Delta\omega}{\omega_{1/2} R} \tag{4.12}$$

Transformed back into time domain leads to an operator $\mathcal{O}$:

$$\mathcal{O} = \frac{1}{\omega_{1/2} R}\left((\omega_{1/2} + i\Delta\omega) + \frac{\mathrm{d}}{\mathrm{d}t}\right) \tag{4.13}$$

This operator can be applied to the measured deviation from the desired setpoint. The result has to be added to the previous feedforward table. A more detailed description of this algorithm is given in section 5.4.7.

Chapter 5

The Digital RF Control System

The digital control system regulates the real and imaginary part of the accelerating field. Since it is impractical to sample an RF field with a frequency of 1.3 GHz field detectors are used that measure the envelope of the RF field. The signals from the detectors can be digitised and send to a DSP. The DSP processes these data and calculates the control signals. These signals are used to modify the RF wave sent to the cavity. In this chapter the hardware of the digital control system and the used algorithms are described. At first the function principle, advantages and performance of the different field detectors is investigated. Then the algorithms of the control are described and finally the modulation of the incident wave is illustrated.

5.1 Requirements

As mentioned in chapter 2.1 in the VUV-FEL the SASE-effect is used to generate a laser beam. To start the SASE process the electron density in one bunch has to be very high. This means the bunches have to be compressed in longitudinal and transversal direction. The longitudinal bunch compression is done in a dispersive (energy depending) chicane. To have the right compression it is crucial that the energy distribution in the electron bunch precisely adjustable. This can only be achieved, if the amplitude of the accelerating field and the phase at which the electrons are inserted into the cavity are stable. Simulations have been done that lead to the requirements for the field stability.

Results of simulations concerning the injector area of the linac up to the first bunch compressor are given in [13]. The relative error in the amplitude of the field in the gun resonator has to be below 0.5 %. The phase of the field must be stable within a range of $\pm 2^\circ$. Start-to-end (S2E) simulations in the

linac layout for the European XFEL project[1] lead to tighter requirements for the phase stability of at least 0.5° [18].

5.2 The Field-Detectors

To control of the field in the gun cavity the incident and reflected RF wave has to be measured and monitored very precisely. The envelope of the field as defined in section 3.3 contains all informations about the amplitude of the measured field and its phase compared to that of a master oscillator with the same frequency (1.3 GHz). Thus it is enough to measure the envelope. It is described by a complex number (with amplitude and phase).

The envelope is measured using different field detectors. The signals from the detectors are sampled digitally. The sampling frequency is 1 MHz except for the phase detector AD 8302 (see below) which is sampled with 9 Mhz.

For the detection of the envelope of the incident and the reflected rf waves field various detectors are used. They are described in the following. The same set of field detectors is used for the forward and the reflected RF field. Except for one kind of field detectors, the downconverters, all detectors are put into one box (see figure 5.1). This box is connected to the two outputs of the directional coupler (forward and reflected rf wave) and to the master oscillator providing the reference frequency of 1.3 GHz. These input signals are distributed to the field detectors inside the box and attenuated according to the required input levels of the detectors. A scheme of the power distribution inside the box and a block scheme of the box are presented in appendix B. The outputs of the detectors are connected to differential amplifiers. Their differential outputs are sent to connectors at front plane of the detector box and from there to the analog to digital converters (ADCs).

In this section the different detectors are described and tests of their performance and results are presented. The whole power distribution and the output amplifiers are all included in the tests. The given output and input levels refer to the detector box and not to the detectors itself.

5.2.1 The IQ Detector AD 8347

For the feedback control of the field the AD 8347 IQ detector is used. I stands for in phase, Q for quadrature. An IQ detector measures the envelope of the rf field as a complex number and delivers values proportional to the real (I) and the imaginary (Q) part of this number. Since the complex number contains a phase this detector needs an input from the master oscillator as

[1] Since the VUV-FEL is used as a test facility for the XFEL in addition to the use of the generated laser beam this requirements are also considered here.

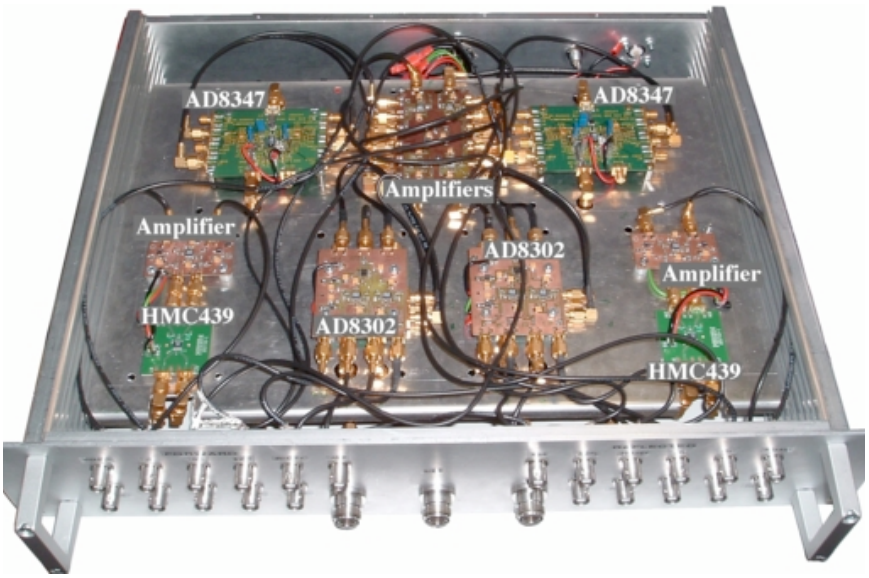

Figure 5.1: Photograph of the detector box for the gun control. (Detector diodes to measure the amplitude of the forward and reflected rf waves are also inside the box, but they can not be seen on the photograph.)

reference (LO input) in addition to the input for the field to measure (RF input).

In the IQ detector the RF signal is split and multiplied by a mixer with two signals from the master oscillator with a 90° phase shift between them. The LO input signal is split by a hybrid power splitter which provides a 90° phase shift between the outputs (figure 5.2). Multiplying two signals with the same frequency ($A\cos(\omega t)$ and $B\cos(\omega t+\phi)$) yields:

$$A\cos(\omega t)\cdot B\cos(\omega t+\phi)=\frac{AB}{2}\Big(\cos(\phi)+\cos(2\omega t+\phi)\Big) \qquad (5.1)$$

The second term has a high frequency (twice the frequency of the inputs) and can be filtered out very easily by a lowpass. The output is proportional to the amplitude A of the RF signal and the cosine of the phase difference ϕ between the RF and the LO input.

If the field from the master oscillator is $B\cos(\omega t)$ and the RF field to be measured is $A\cos(\omega t+\phi)$ the two outputs I and Q of the IQ detector are:

$$I=\frac{AB}{2}\cos(\phi) \quad \text{and} \quad Q=\frac{AB}{2}\cos(\phi-90^\circ)=\frac{AB}{2}\sin(\phi)$$

I and Q are the real and imaginary part of the complex number $\frac{AB}{2}e^{\mathrm{i}\phi}$. The input amplitude from the master oscillator is kept constant, so that the output amplitude is a measure of the RF amplitude. If the frequencies

of the two inputs of the detector (RF and LO) are slightly different (up to 1 MHz) the phase shift between them can be viewed as slowly changing and the outputs will oscillate with the frequency difference of the two inputs.

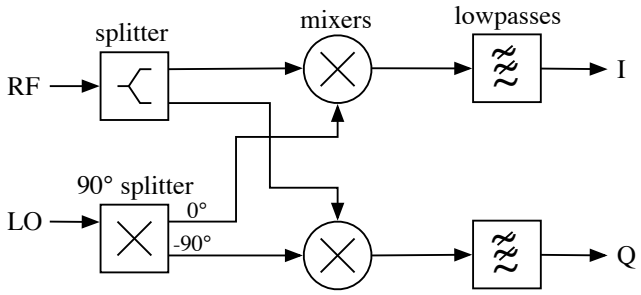

Figure 5.2: Principle of the IQ detector

The detector is mounted on an evaluation board from Analog Devices. A description of this board is given in the data sheet of the detector [3]. The AD 8347 has one differential output and one bipolar output for each, the I and the Q values. Measurements show that the internal differential amplifiers have a high noise level, so we decided to use the bipolar outputs and connect them to external differential output amplifiers (AD 8138). The evaluation board is equipped with an offset control. This control assumes that all Fourier components of the output signals with frequencies below 400 Hz are caused by the offset and they are filtered away. Since the field changes during flat top are slow, this offset control can not be used. In figure C.2 in appendix C a circuit diagram of this setup is given.

As an alternatively to detecting the real and imaginary part, the amplitude and phase can be measured. The disadvantage of this method lies in the phase detection. Since the phase is periodical there is either a jump between $-180°$ and $180°$ in the characteristic of the phase detector causing uncertainties near $180°$ of phase shift, or the characteristic is symmetric around $0°$ so that positive and negative phases can not be distinguished. Moreover, the phase detection is problematic for low amplitudes, because the phase becomes undefined if the amplitude approaches zero (the tangent of the phase is the tangent of the imaginary part divided by the real part, $\tan\varphi = \frac{\text{imag}}{\text{real}}$. Both approach zero).

A prerequisite for the functioning of the IQ detector is that the $90°$ phase shift inside the detector has to be very precise and the two output amplifiers must be exactly equal to get real and imaginary part with the right relative values (low IQ-imbalance).

A different problem is that the detectors have offsets which must be measured and subtracted. This is only possible if the offsets are stable.

According to the data sheet of the detector AD 8347 [3] the IQ-imbalance is 0.8°, which is better than the requirement for the control (see section 5.1).

The noise level is checked by splitting a signal from one generator with a power splitter and connecting it to both inputs of the detector (see figure 5.3). The outputs of the detector are put to an oscilloscope and to a dynamic signal analyzer. The noise of the signal generator is not seen in this setup, because it will be the same on both inputs of the detector and thus cancel itself for the most part.

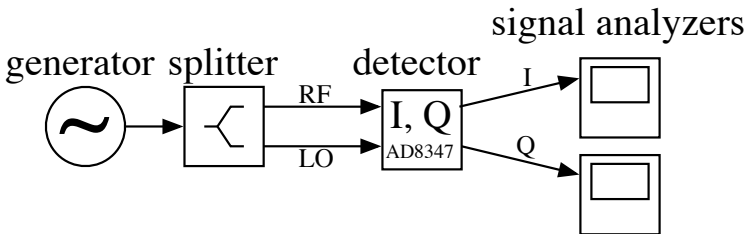

Figure 5.3: Setup of the noise measurement

This noise measurement has been done with the detector AD 8347 being installed in the detector box, including all attenunators, power splitters and the output amplifiers. The noise level is about $1.5\,\mathrm{mV_{pp}}$ compared to a signal level of up to $1\,\mathrm{V_{pp}}$. The measured noise spectrum is shown in figure 5.4. It is at $1.5\,\frac{\mu\mathrm{V_{rms}}}{\sqrt{Hz}}$ for all frequencies. The noise spectrum shows no peaks after the temperature control of the detector box was turned off (with the internal temperature control harmonics of 50 Hz could be seen). The detector box is put in a temperature stabilised rack, so we will not use the temperature stabilisation of the box in the future to avoid this additional noise source. The results for I and Q look the same. The noise level of the IQ detector is $0.1\,\%_{\mathrm{rms}}$ of the output signal. This level is low enough to measure the rf field with a precision that is sufficient to reach the requirements for the field stability inside the gun.

The IQ imbalance can be measured by connecting two frequency generators to the inputs of the detector. The generators are slightly detuned with respect to each other. The output of I and Q should be two sinusoidal curves with a phase difference of 90°. The frequency of the sine curves is the frequency difference between the two oscillators. The expected result when plotting the I output against the Q output is a circle with a diameter proportional to the amplitude of the RF input. Such circles can be seen in figure 5.5 for different amplitudes. The deviation from a perfect circle is about the same as the noise floor.

The linearity of the detector can be checked by plotting the diameter of the circles against the amplitude of the incident signal. This is shown in

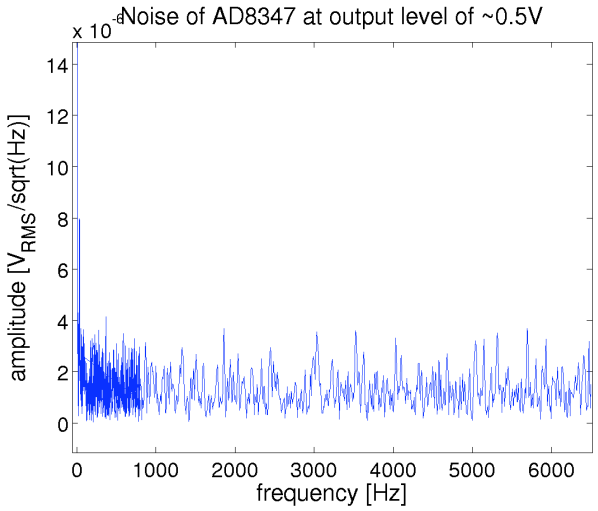

Figure 5.4: Noise spectrum of the IQ detector AD 8347

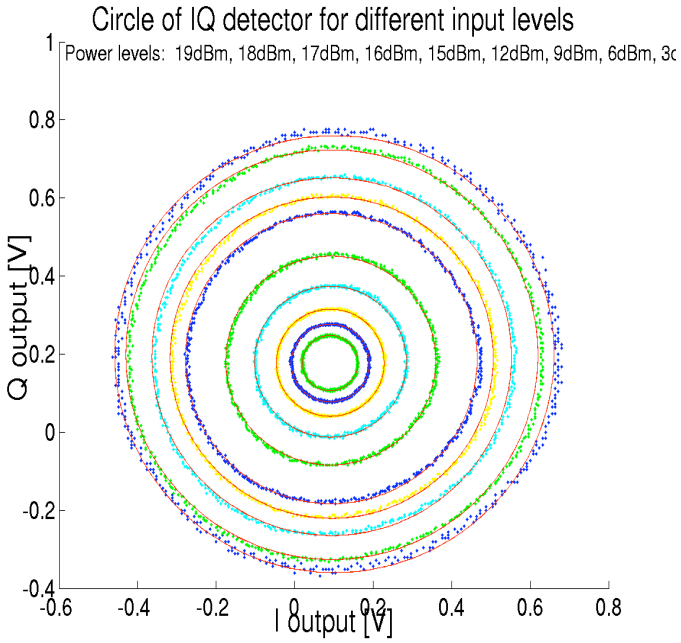

Figure 5.5: If two generators with different frequencies are connected to the inputs of the detector, the output should be a circle in the complex plain. The red circles are ideal circles.

figure 5.6. Below an input level of 18 dB_m no nonlinearity can be seen. The deviation from a straight line at high power is an artifact of the generator. It can be observed with the other detectors, too (see below in this chapter). During normal operation we will not reach the input power levels of 18 dB except for the spikes of the reflected power.

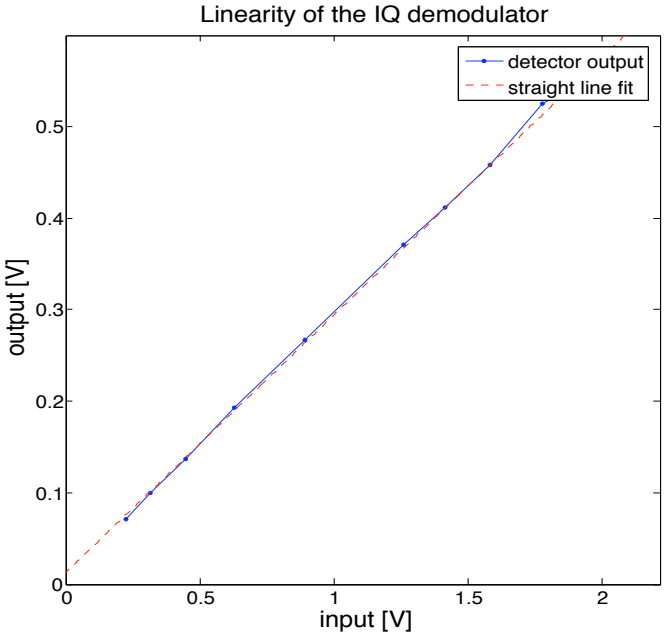

Figure 5.6: Results of the linearity measurements of the IQ detector

The temperature dependance of the detector has been checked. It is about 20 $\frac{mV}{°C}$. Since the detectors are placed in a temperature stabilised rack this temperature dependance does not cause problems.

All these measurements have been done with the IQ detector installed in the control box with the other detectors. The power and voltages referred to in the figures 5.5, 5.4, and 5.6 are those at the connections of the box, not directly at the detectors.

The noise floor of the detector with the used output amplifiers is low enough to resolve deviations of the field of below the requirements of 0.5 % in amplitude and 2° in phase. Thus the detector is suitable to reach the required field stability (see 5.1) for the VUV-FEL.

5.2.2 The Logarithmic Gain and Phase Detector AD 8302

Measurements of the power that is emitted by the cavity directly after the incident power has been turned off are done with the gain and phase detector AD 8302. At the inputs the AD 8302 field detector gets a 1.3 GHz

reference from the master oscillator (LO input) and the signal from the directional coupler (RF input). One of the two output signals is proportional to the phase between the two input signals. The phase measurement is done by multiplication in an analogue mixer. Let the field at the RF input be $A\cos(\omega t + \phi)$ and at the LO input be $B\cos(\omega t)$. The mixer multiplies these fields and applies a lowpass filter to remove the term with the sum frequency (see equation 5.1). The output signal is proportional to $\cos(\phi)$. Before reaching the mixer the input amplitudes are limited to keep them constant.

The second output of the AD 8302 is proportional to the gain between the LO and the RF input signal (i.e., the logarithm of the ratio of the RF and the LO input signal). The gain is measured by sending both input signals into logarithmic amplifiers. Then the logarithms of the signals are subtracted from each other. The output signal V_{out} is proportional to the difference of the logarithms of the input amplitudes:

$$V_{\text{out}} \propto \log(A) - \log(B) \tag{5.2}$$

For a constant amplitude at the LO input the detector can be used as an amplitude detector.

The AD 8302 can measure signals at the RF input with a power of 30 dB higher or lower than the signal at the LO input. This big dynamic range makes it possible to measure the decay of the cavity field after the incident power from the klystron has been turned off although the time constant is only $\tau = 2.7\,\mu$s. With the high dynamic range of the detector and with a sampling rate of 9 MHz of the ADC we get more than 50 sampling points before the field is decayed below the measurable level.

This detector chip is mounted on an evaluation board from Analog Devices [2].

The quality factor and the detuning of the cavity can be determined from the field decay. How this is done will be described in the next section. This means that rapidly changing signals have to be measured. To do this the output bandwidth has to be high. Since this detector is sampled with 9 MHz, the output bandwidth should be at least 5 MHz otherwise changes of the signal levels between two sampling points could be strongly reduced by the lowpass character of the output. The noise floor and the output bandwidth have been measured. According to the data sheet [2] the nominal precision of the amplitude measurement is 1 % and the precision of the phase measurement is 0.8°.

A noise measurement of this detector was done by connecting a signal generator to the LO input and a termination to the RF input. The result is shown in figure 5.7. The noise floor is sufficiently low ($\approx 20\,\frac{\mu\text{V}_{\text{rms}}}{\sqrt{\text{Hz}}}$), since no high precision measurement is planned with this detector, but it is much higher than one would expect from the data sheet ($\approx 1\,\frac{\mu\text{V}_{\text{rms}}}{\sqrt{\text{Hz}}}$), suggesting

that the output amplifiers are the main noise sources. Harmonics of 70 Hz can be seen. Their origin has not yet been identified.

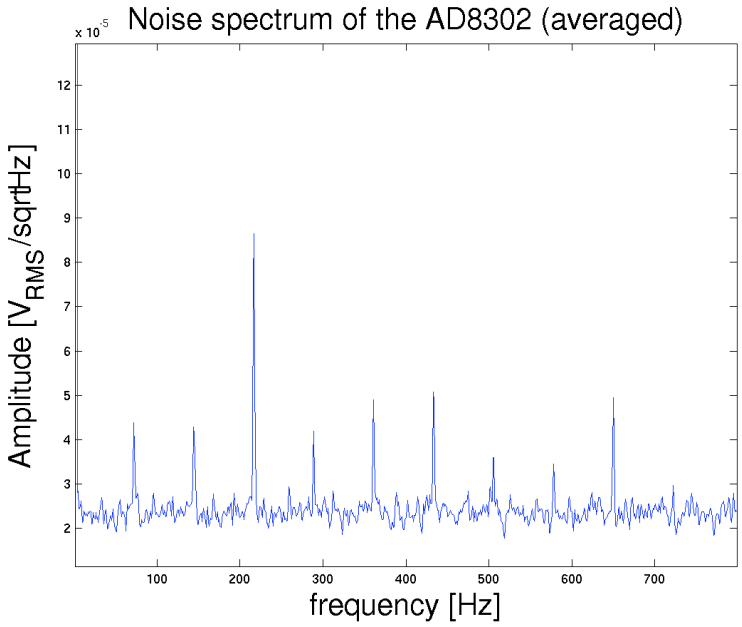

Figure 5.7: Noise spectrum of the AD 8302 amplitude and phase detector

A crosstalk between the phase output and the amplitude output can be seen, if two generators with slightly different frequencies (less than 10 MHz frequency difference) are connected to the LO and the RF input (see figure 5.8). This crosstalk restricts the amplitude resolution of the detector to $\pm 3.5\,\%$.

To estimate the output bandwidth we connected a frequency generator with a constant frequency and amplitude to the LO input. The signal of another generator was sent to the RF input. The frequency of the phase output is the difference in frequencies between the LO and RF input signals. This difference was changed by altering the frequency of the RF input signal. Up to a frequency of 3.3 MHz at the output the amplitude of the phase output is reduced by only 17 % so an output bandwidth of about 10 MHz could be expected. When the output frequency is increased further than 3.6 MHz, the amplitude of the frequency output suddenly increases. If the output frequency is reduced again, it jumps back when the frequency becomes lower then 3.3 MHz. This behavior is shown in figure 5.9. Since the detuning of the gun is not bigger than the bandwidth (60 kHz) normally this does not matter. (The detuning of the gun equals the output frequency of the detector during decay time.) Only directly after turning off the incident power strange readings may occur since the output of the directional coupler

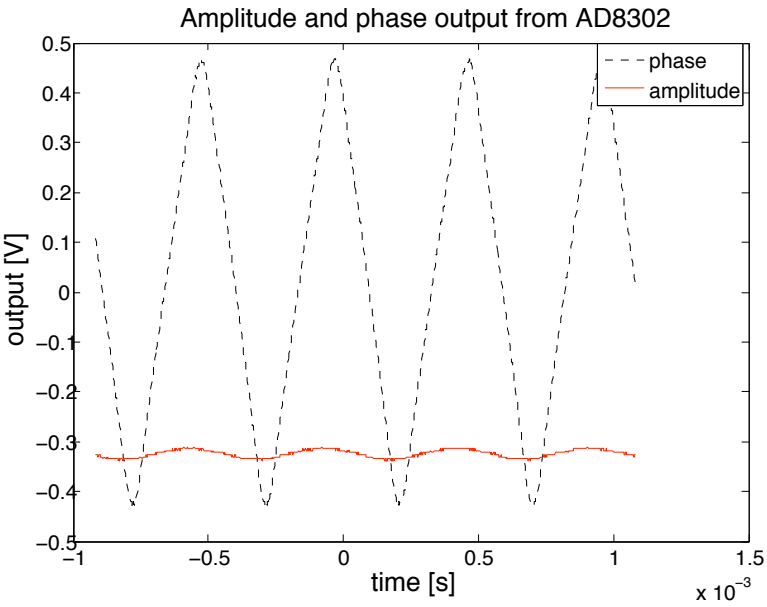

Figure 5.8: Crosstalk between the amplitude and the phase output of the AD8302

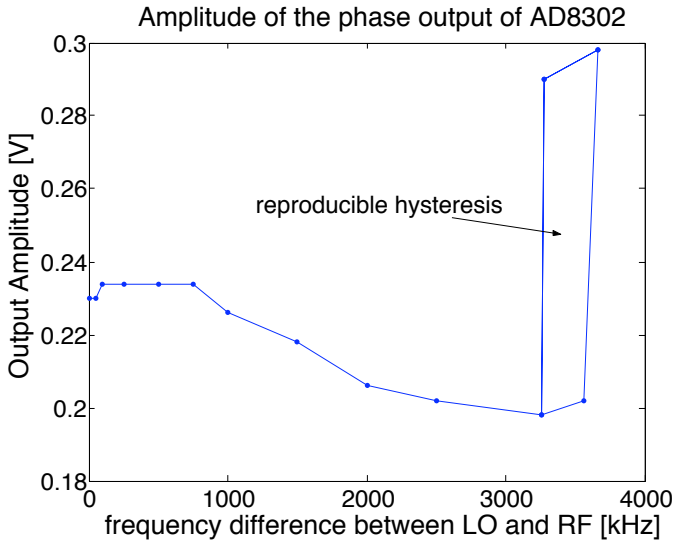

Figure 5.9: Frequency dependence of the phase output of the AD 8302

has high frequency components at this time. The first sample point of the field decay should be omitted in calculations.

The linearity of the AD 8302 detector to the logarithm of the input amplitude was tested, including the power distribution in the detector box and the output amplifier (see figure 5.10). The power levels refer to the box in- and outputs, not directly to the detector. The linearity is very good. The deviation from exact linearity is less than the noise floor. The figure shows the error of the generator at around 18 dB_m which has been observed with the IQ detector before (previous section).

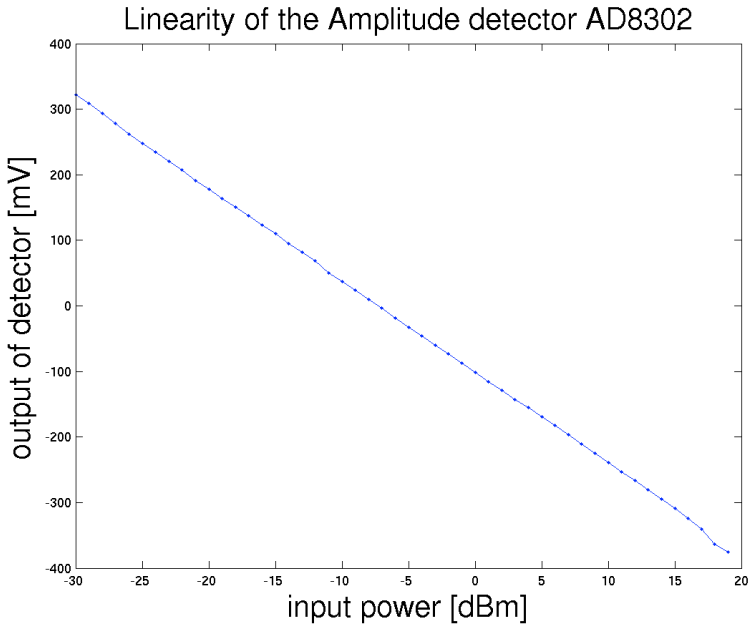

Figure 5.10: Output characteristic of the logarithmic amplitude output of the AD 8302

It follows from these tests that the AD 8302 is suitable for a measurement of the quality factor (about $\pm 1\,\%$) and a measurement of the detuning of the cavity, but high precision measurements can not be made. The big dynamic range of the detector makes it very suitable for the measurement of the decaying field.

5.2.3 The Digital Phase Detector HMC 439

The HMC 439 digital phase detector from Hittite is used to monitor the phase of the incident and the reflected field relative to the master oscillator.

The HMC 439 has an internal flip-flop. This flip-flop is turned to one when the signal from the RF input has zero phase (i.e., the voltage crosses

zero, coming from negative values) and it is turned back to zero by the second input signal (LO input) (see figure 5.11). The mean value over the time is proportional to the phase difference between the two input waves.

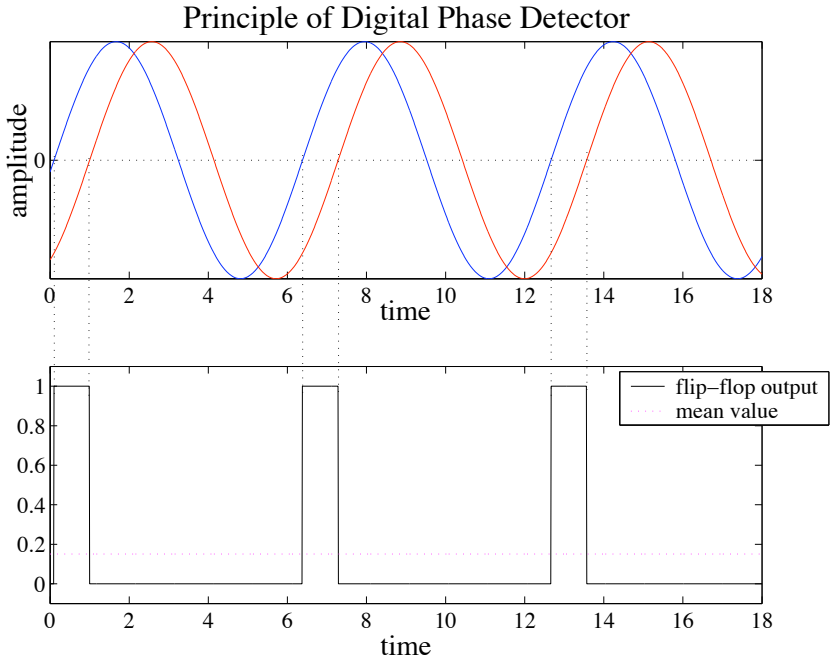

Figure 5.11: A digital phase detector has a internal flip-flop that is switched on by the first sine wave and turned off by the second. The mean value of the flip-flop is proportional to the phase difference of the input signals.

Hittite provides evaluation boards for this detector (see [9]) which we use unchanged. The output of the detector is connected to a differential amplifier with an amplification of two. A circuit diagram of this amplifier is given in appendix C.

The HMC 439 features a very low noise floor and a high linearity of the measured phase. By using two signal generators the characteristic of the detector was measured (see figure 5.12). As expected from the specifications the detector has a good linearity (deviations from perfect linearity are below 1°) except near the phase jump from 180° to −180°.

The noise level was measured with a termination at the RF input. The noise spectrum is shown in figure 5.13. The figure shows an average of 20 noise spectra. The noise is low enough for precision measurements. It is about 400 $\frac{\mathrm{nV_{rms}}}{\sqrt{HZ}}$ at a signal level of 1.5 $\mathrm{V_{pp}}$. According to the data sheet [9] the noise level is 400 $\frac{\mathrm{nV_{rms}}}{\sqrt{HZ}}$. This and other measurements with the same detector suggest that the measured noise floor is due to the output amplifier

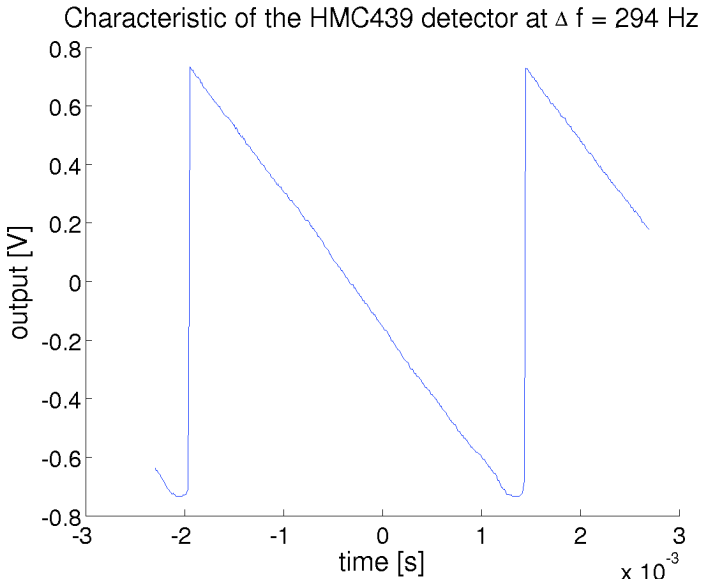

Figure 5.12: Output characteristic of the phase detector HMC 439

rather than the detector itself. With another amplifier the performance might be improved if it should become necessary.

This phase detector is used to monitor the field independently of the IQ detector. The high precision allows to determine clearly if the required phase stability of the fields is maintained as long as we are not near the phase jump at $\pm 180°$.

5.2.4 The Detector Diode ODS 0509 A

The detector diode ODS 0509 A from Omniyig is used to measure the amplitude of the fields independent of the master oscillator (forward and reflected). The output of the diode is proportional to the field amplitude for low input power and proportional to the power (i.e., to the square of the amplitude) for higher power levels.

Unnoticed errors in the field control due to errors from the master oscillator or the distribution of its signal can be ruled out since the diode requires no reference input.

The diode needs quite high input power ($0\,\mathrm{dB_m}$ to $20\,\mathrm{dB_m}$). During the first run of the accelerator the input levels have been too low. The output level into $50\,\Omega$ was about 50 mV, a level of 1 V is optimal. No signal could be seen with the ADC. The detector box has been reconstructed since then to have higher power levels at the diodes during the current run of the VUV-FEL.

The characteristic of the diode has been measured with a signal generator

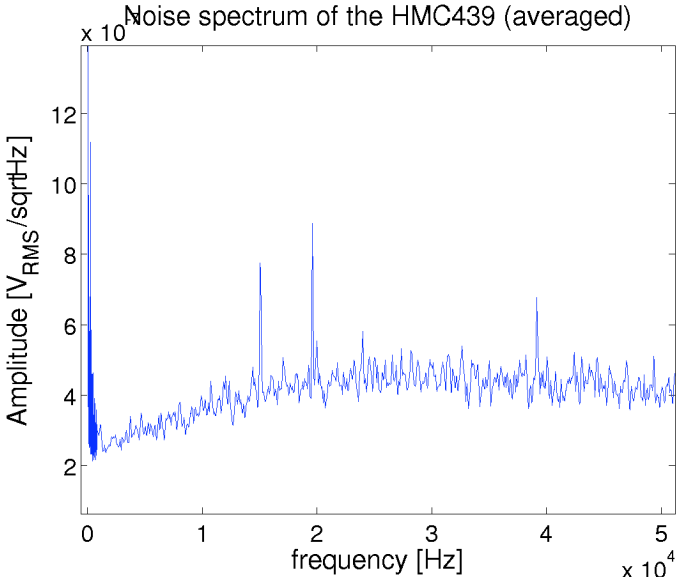

Figure 5.13: Noise level of the phase detector HMC 439 in frequency domain

(see figure 5.14).

After the reconstruction of the power distribution inside the detector box the output of the detector diode is linear to the amplitude of the input power during flat top.

5.2.5 The Downconverter

In contrast to the detectors mentioned above the downconverters are not installed inside the detector box, but on extra boards. With the downconverter real (I) and imaginary (Q) part of the envelope of the field are measured, but in contrast to an IQ detector the downconverter doesn't multiply two signals with the same frequency to get a DC output.

The principle of the downconverter is based on the conversion of the 1.3 GHz signal to a signal with an intermediate frequency of 250 kHz which can be sampled to get the real and imaginary part. To do such a downconversion the RF field to be measured ($V_{\mathrm{RF}} = A\cos(\omega t + \phi)$) is multiplied by a mixer with a reference with 250 kHz higher frequency than the signal frequency ($V_{\mathrm{LO}} = B\cos(\omega_{\mathrm{LO}} t)$). The result is a wave with the intermediate frequency of 250 kHz which contains the information of amplitude and phase of the RF field:

$$V_{\mathrm{IF}} = \frac{AB}{2}\cos\left((\omega - \omega_{\mathrm{LO}})t + \phi\right) \tag{5.3}$$

This intermediate field is sampled by an ADC with a frequency of 1 MHz. Thus four samples with 90° phase shift between them are taken every period.

These four sampling points are interpreted as I, Q, -I and -Q in succession.

The advantage of this detection scheme is that DC offsets do not cause problems, because the a wave with 250 kHz is sampled and not a DC signal. The DC offset V_{DC} can always be found from the measured signals using the formula $V_{\mathrm{DC}} = \frac{\mathrm{I}+(-\mathrm{I})}{2}$ or $V_{\mathrm{DC}} = \frac{\mathrm{Q}+(-\mathrm{Q})}{2}$. However, the vector modulator has to rotate the reference signal very precisely by 90° while the amplitude must not be changed. Since the precision of the rotation is only about $\pm 1°$ and there is a 1 MHz ripple on top the signal from the downconverter. Some effort is done to improve this, but the remaining ripple is still about 1 % of the output level. Another for the gun control even more important disadvantage of the downconverter is that real and imaginary part of the wave are measured only once every 2 μs. Comparing this with the time constant $\tau = 2.7\,\mu$s of the gun cavity shows that the field can change quite a lot between two data points. For that reason the downconverter is not used for the field control. It is only used to verify signals measured with the other detectors to find error sources if problems with the other detectors should occur.

Signals from the downconverters have been saved during the first run of the VUV-FEL. From this signals single curves for +I, -I, +Q, and -Q have been generated. Figure 5.15 shows this curves taken from the incident wave during one pulse.

We observe an overshoot and a field decay with a big time constant. The pulse from the klystron is nearly rectangular; the field from the klystron decays much faster then one microsecond. The observed artifacts of the detector have the same signs for all four signals. Unfortunately, the overshoot for +I and -I, respectively +Q and -Q are not the same. Even using the formula $\mathrm{I} = \frac{(+\mathrm{I})\ -\ (-\mathrm{I})}{2}$ does not lead to a cancellation of this error.

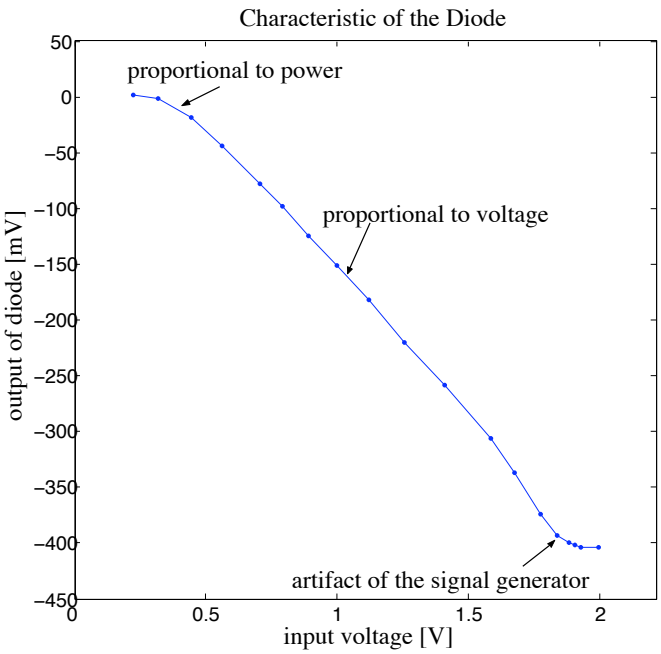

Figure 5.14: Characteristic of the detector diode ODS 0509 A inside the detector box

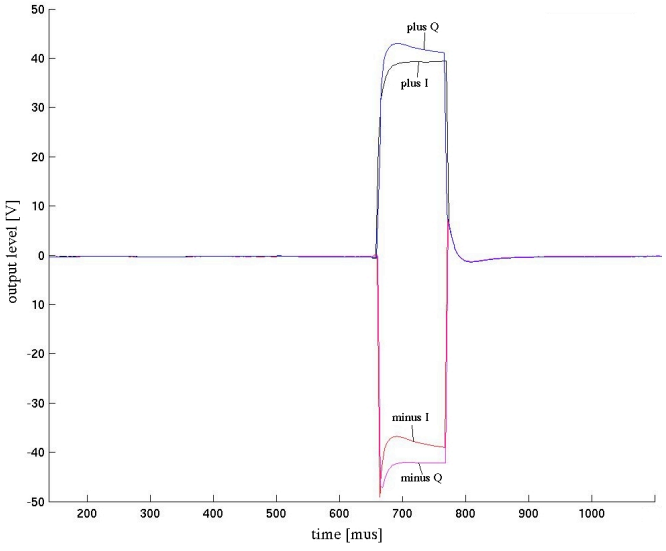

Figure 5.15: Reconstructed signal of one RF pulse from the klystron measured with the downconverter

5.2.6 Summary

In table 5.1 the performance of the detectors and their purpose in the control system is summarized.

Name	**Output Property**	**relative error (rms)**	**Comments**
AD 8347	I and Q	$\pm 0.1\,\%$	Precise IQ detection, no direct phase detection needed. Used for the feedback control.
AD 8302	log(A) phase	$\pm 3.5\,\%$ $\pm 1^\circ$	High output bandwidth, high dynamic range. Used for the measurement of the quality factor and the detuning
HMC 439	phase	$\pm 0.5^\circ$	High precision, low noise phase detector. Used for monitoring.
ODS 0509 A	Amplitude		Independent of the master oscillator. Used for monitoring.
Down-converter	I and Q	$\gtrsim 1\,\%$ ripple, overshoot	Full information about the wave only at a rate of 500 kHz. Currently only backup system.

Table 5.1: The detectors and their performance and use in the control system

5.3 Measurement of the Detuning and the Quality Factor

After the power from the klystron is turned off at the end of each pulse, the amplitude of the field emitted by the gun cavity is proportional to the field inside the cavity. The field emitted from the cavity is handled by the directional coupler as the reflected field. As seen in section 3.3 the field decays exponentially $A(t) = A_0 \cdot e^{-\frac{t}{\tau}}$. Using $Q_L = \frac{\tau\omega_0}{2}$ (equation 3.26) from this follows:

$$\begin{aligned} & A(t) = A_0 \cdot e^{-\frac{t}{\tau}} \\ \Leftrightarrow \quad & \ln(\frac{A(t)}{A_0}) = -\frac{t}{\tau} \\ \Leftrightarrow \quad & \frac{d}{dt}\Big(\frac{A(t)}{A_0}\Big) = -\frac{1}{\tau} \\ \Leftrightarrow \quad & Q_L = -\frac{\omega_0}{2\frac{d}{dt}\big(\frac{A(t)}{A_0}\big)} \end{aligned} \tag{5.4}$$

By using a logarithmic field detector it is easy to determine the loaded quality factor of the gun resonator by fitting a straight line to the measured field decay and determining its slope (see figure 5.16).

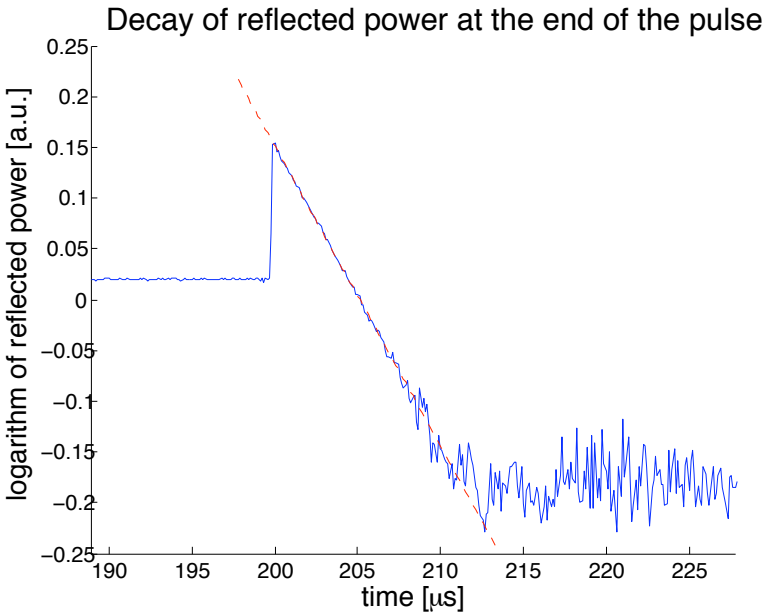

Figure 5.16: Reflected field at the end of the rf pulse

The detuning $\Delta\omega$ can be found from the phase ϕ_r of the reflected wave relative to the master oscillator after the klystron is turned off. Without the exiting power from the klystron the field in the gun cavity oscillates with the resonance frequency ω_0 of the cavity at that moment. In this case the change in phase relative to the master oscillator is linear in time. The time derivative of the phase is the detuning:

$$\Delta\omega = -\frac{d\phi_r}{dt}$$

By determining the slope of the measured phase during the field decay the detuning of the gun resonator can be measured. The phase at the end of one pulse and a straight line fitted to it are shown in figure 5.17.

Note that for this measurement only the phase change is observed, not an absolute phase value. Thus it is possible to measure the detuning without the correction of phase shifts in cables, waveguides, etc.

5.4 Algorithms

5.4.1 Calibration of the Detectors for the Forward Power

The field detectors convert amplitude or phase of the envelope of the signals at their inputs to a corresponding voltage. Before the signal reaches the detectors it is attenuated and shifted in phase by the wave guides, couplers,

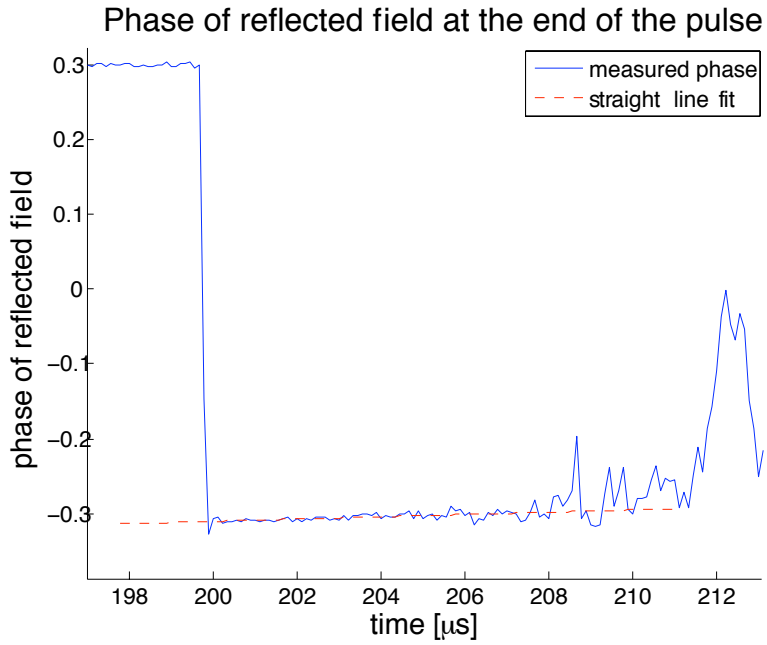

Figure 5.17: Phase of reflected field at the end of the rf pulse

attenuators and power splitters it passes. ADCs convert the output voltage of the detectors to digital numbers. These numbers can be calibrated in software to get the correct values of the forward and the reflected power at the input coupler of the gun.

Offset Compensation

If the incident wave is zero the outputs of the IQ detector should also be zero. To adjust offsets on I and Q, the detector chip has inputs (IOFS and QOFS, see figure C.2 in appendix C) where a voltage can be applied. We have been able to reduce the offset to a few percent of the maximum output level. The rest has to be adjusted in the software after the digitisation by adding a constant to the measured values. This constant is the minus one times the output value of the detector when the forward power is turned off.

Amplitude Calibration

To calibrate the detectors that measure the amplitude of the incident field we have a power meter which measures the peak power during one pulse. With this power meter I and Q can be calibrated separately by changing the phase of the incident wave such that only I respectively Q shows a value different from zero. This way the detectors will be calibrated to show

$\sqrt{\text{MW}}$. A calibration in MV/m corresponding to the accelerating gradient of the field inside the cavity can be done after the energy of the beam has been measured in a dispersive section (i.e., the path of the electrons depends on the energy) of the accelerator behind the gun.

The output of the detector diode is proportional to the incident power for low input power and proportional to the field amplitude for higher input power (see chapter 5.2.4). Thus a linear calibration is not precise. The diode is more used for qualitative monitoring. It is also calibrated using the power meter with the assumption of high input power.

Since the zero of a logarithmic detector is not defined ($\ln(0) = -\infty$) the power meter is not sufficient to calibrate the logarithmic amplitude output of the AD 8302 detector. After the IQ detector is calibrated in amplitude, its output can be used to calibrate the logarithmic detector.

Phase Calibration

The calibration factor between the phase and the output voltage of the AD 8302 is determined by putting a microwave source with a slightly different frequency (about 1 kHz higher or lower) than the reference to the rf input. The phase between these two signals changes constantly with the time. The output is the triangular characteristic of the detector (see figure 5.18). The range of the oscillation from bottom to top is known to be 180°. Since the phase detection is not good near ±90° for a good calibration a line has been fitted to the output signal between −80° and +80° to create a triangular signal with 180° phase shift between the maximum and the minimum (see figure 5.18). The 0° point can be defined the same way as with the IQ detector (see below).

With the same setup as used for the phase calibration of the AD 8302, the output of the HMC 439 is a sawtooth shaped signal (see figure 5.12). The amplitude corresponds to a frequency change from −180° to +180°.

The phase of the envelope of the microwave is only defined relative to a reference. This reference should be given by the electron beam. The phase of the field in the gun cavity where the beam has the maximum acceleration (on crest acceleration) is defined as zero. This calibration can be done by sweeping through the phase of the forward wave and looking at the beam energy. When the detuning of the cavity is zero the phase of the incident wave is the same as that of the field inside the cavity. This way the zero of all phase dependent detectors (phase detectors and IQ detector) can be determined.

5.4.2 Calibration of the Detectors for the Reflected Power

The reflected power can not be calibrated with the use of a power meter as described for the forward power, because the reflected power has short

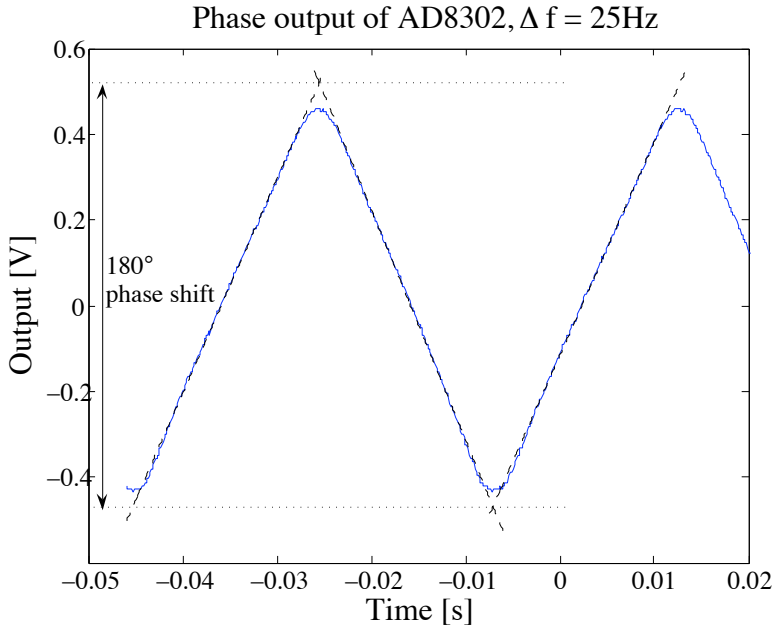

Figure 5.18: Characteristic of the phase output of the AD 8302 with lines fitted to the slopes to determine the phase calibration of the detector

peaks at the beginning and the end of each pulse. The peak power of the reflected wave changes significantly within nanoseconds. This can not be resolved with the power meter and with the detectors. Thus the peak is truncated and can not be used for a proper calibration.

We would like to have a calibration that allows us to calculate the field in the cavity as the complex sum of the forward and the reflected wave ($V_{\text{for}} + V_{\text{ref}} = V_{\text{cav}}$).

If the gun is tuned well, the detuning is zero at one time during the pulse. At this instant the reflected wave is shifted by 180° in phase compared to the incident wave (the angle α in figure 5.19 is zero if $\psi = 0°$) and its amplitude is minimal. By looking at the amplitude of the reflected power this time can be found easily. This way one point where we know the phase of the reflected wave relative to the incident wave is found and thus the phase of reflected wave can be calibrated.

During the flat top the forward power is six to seven times bigger than the reflected power; after the incident wave is turned off only reflected power is measured. The logarithm of the field amplitude in the cavity is constant during the last microseconds of the pulse and decays linearly from this level when no incident power reaches the cavity. The field reconstructed from the forward and reflected wave rises at the end of the pulse if the calibration factor of the reflected wave is too big and drops too fast in the first microsecond

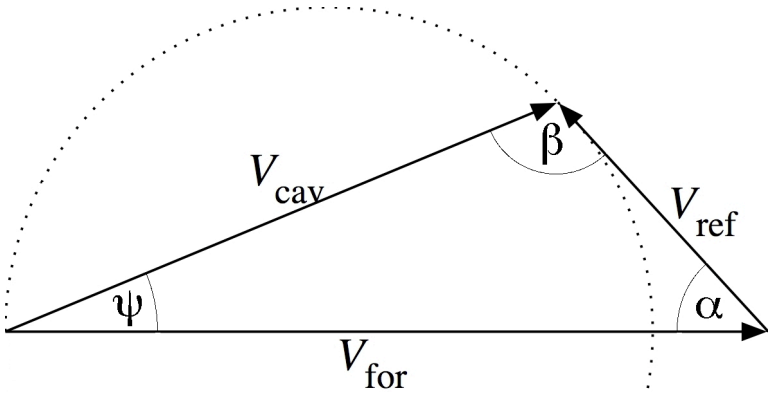

Figure 5.19: Vectors of the forward, reflected and cavity field

if the calibration factor is too small. The linearly decaying logarithm of the reflected power must cross the point of the flat top where the incident power is turned off (see figure 5.20). This way the absolute value of the calibration

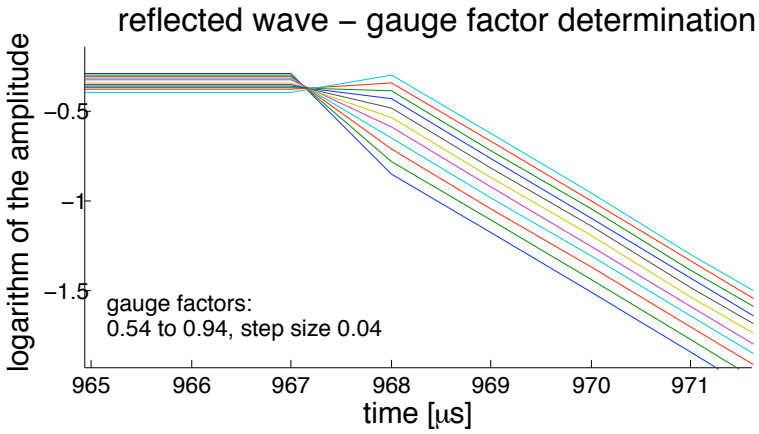

Figure 5.20: Reconstructed cavity field at the end of the pulse with different calibration factors.

factor for the reflected wave can be found and the field in the cavity can be reconstructed (see figure 5.21).

To find this factor exactly the time when the incident power is turned off has to found precisely. With the IQ detector the time resolution is only 1 μs and the calibration will have an uncertainty of about 25 %. With the help of the rf gate the end of the pulse can be shifted in steps of 111 ns making the calibration a factor of nine more precise (2.8 %). Since the amplitude of the incident wave during flat top is about six times higher than the amplitude of the reflected wave, the cavity field can be reconstructed with a precision

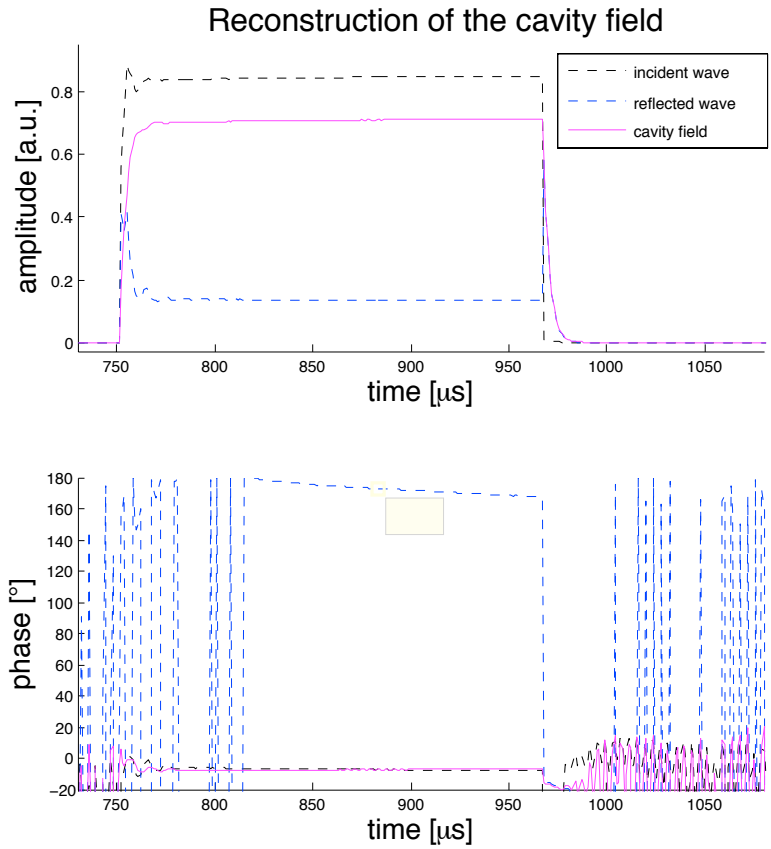

Figure 5.21: Cavity field reconstructed from the measurement of the incident and the reflected wave.

of 0.5 %.

This is only theoretically enough to reach the required 0.5 % in amplitude. To reach the requirements a more precise measurement of the time the forward power is tuned off has to be done. This is possible with the timing system of the VUV-FEL, but it has not been done, yet.

This way of determining the calibration factor between the forward and the reflected wave has the advantage that the crosstalk of the forward power to the reflected power in the directional coupler is included in this calibration factor.

For the calibration many rf pulses can be averaged, thus reducing the detector noise. The precision of the phase calibration is limited by a ripple on the output of the IQ detector which is a crosstalk from the downconverter. This crosstalk is described later (chapter 6.1). The time when the reflected power is minimal can be determined with a precision of $\pm 5\,\mu$s, during this time the phase of the field in the cavity changes by about 0.15°. The ripple

itself has an amplitude of $0.2^{\circ}_{\mathrm{pp}}$, so the point where the reflected wave has a 180° phase shift compared to the incident wave can be found with a precision of $\pm 0.2^{\circ}$.

5.4.3 Measurement of the Detuning During Flat Top

In the stationary case, from the theory the phase difference ψ between the incident field and the field inside the cavity is known in as $\tan(\psi) = \frac{2Q_{\mathrm{L}}\Delta\omega}{\omega_0} = \frac{\Delta\omega}{\omega_{1/2}}$ for a given detuning $\Delta\omega$ (equation 3.25). Since the time constant of the gun cavity is very short ($2.7\,\mu$s) this can be assumed to be valid during the whole flat top.

The detuning at the end of the pulse can be measured by determining the slope of the phase of the reflected wave (see section 5.3) without calibrating any amplitude or defining the zero of the phase. To quantify the detuning at different times of the rf pulse different pulses with the same starting conditions and different lengths are used. At the end of each of the pulses the detuning can be determined and thus the detuning as a function of the time after the beginning of the pulse is worked out, provided that the starting conditions for the different pulses are really unchanged.

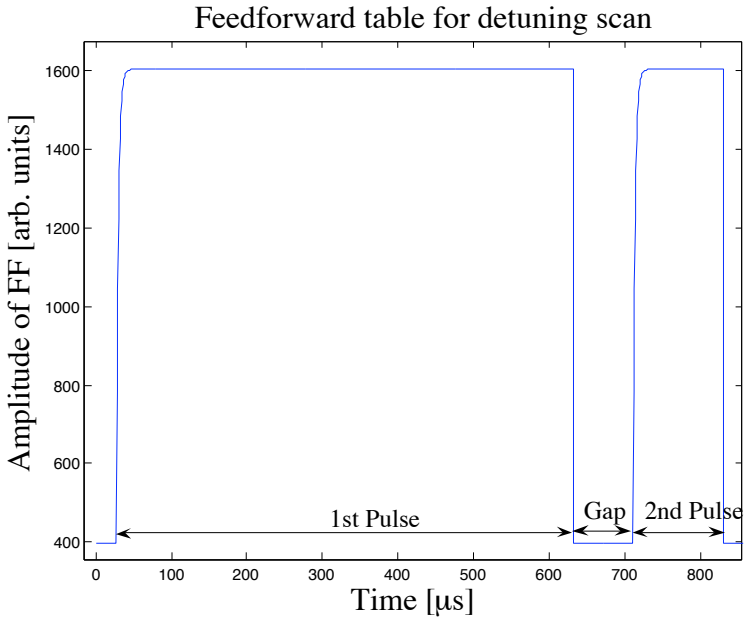

Figure 5.22: Shape of the incident wave for the detuning measurement

If the pulse length is changed the energy dissipated in the gun cavity changes. Even though the cooling can establish the same temperature in the iris of the cavity at the beginning of every pulse it takes a lot of time (about

30 min.) until the temperature has been stabilised after the pulse length was changed and the temperature distribution inside the cavity might be different. To avoid this problem a long rf pulse is split into two pulses with a short gap between them (see figure 5.22).

At the end of the first gap the detuning can be measured. By shifting the gap in time the detuning at any time of the pulse can be determined and the power dissipated inside the cavity is always constant. By calculating the detuning after the second pulse the stability of the conditions can be checked. The result of this measurement is shown in figure 5.23. It turns out that the detuning is changing linear with the field energy in the gun. For a pulse with 600 μs flat top duration and 2.7 MW forward power it changes by 6 kHz. This means the constant to calculate the detuning is about 4 $\frac{\text{Hz}}{\text{MW}\mu\text{s}}$. Having obtained the detuning as a function of pulse duration, the phase

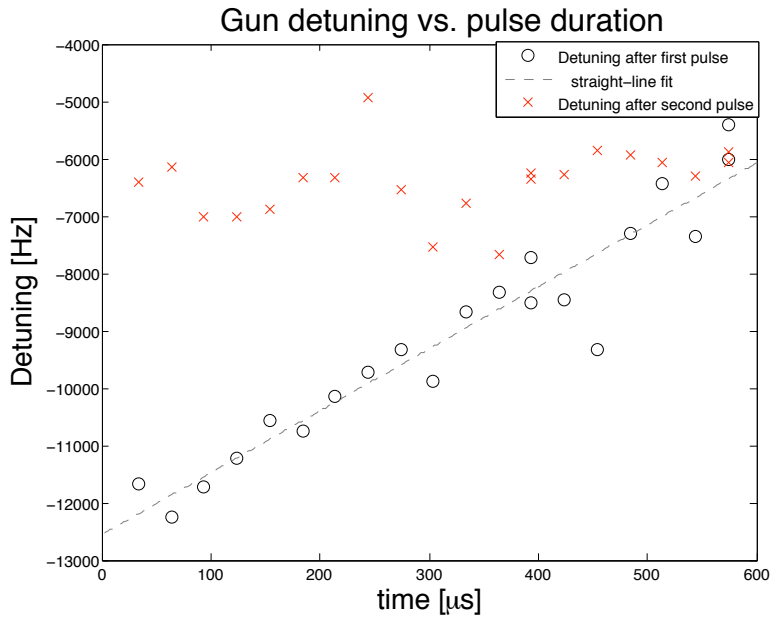

Figure 5.23: Detuning of the gun cavity plotted against the duration of the pulse. The forward power was 2.7 MW

difference between the incident wave and the field in the cavity ψ can be calculated for any time during the pulse. This can be used to verify the calibration of the detectors for the reflected wave.

5.4.4 Calibration of the DSP

It is convenient for the user to be able to set the desired forward power in MW. If this is set to zero the result should be no forward power. To achieve this an offset compensation has to be added to the DSP signal before

it is converted to an analog control signal. This offset compensation is found experimentally simply by searching the settings for I and Q (real and imaginary part) where the forward power has a minimum. The calibration factor which converts the setpoint given by the operator in MW to a digital value in the DSP is also found experimentally. The desired forward power is set into the DSP and then the calibration is adjusted in amplitude and phase until the field measurement corresponds to this setpoint.

In our case we have two calibration factors. One factor is used to convert the digital number in the DSP to the voltage output of the ADC, the second factor converts the ADC output voltage to the power of the field.

5.4.5 Feedforward

The control signals are generated by the DSP in the digital control system. They are converted to analog values by digital to analog converters (DAC) at a rate of 1 MHz and sent to the vector modulator (see below). This implies we can change the incident wave every microsecond. Since the duration of one rf pulse is always below 2 ms, 2048 complex numbers or 4096 real numbers are used to define the form of the driving wave for one pulse.

The feedforward table is a table of 4096 real numbers. The first two values are the values for I and Q for the first microsecond, the 3rd and 4th value are I and Q for the 2nd microsecond and so on.

The simplest feedforward table contains zeros where the forward power is off and a constant value during the filling giving the desired forward power. This table is multiplied by the calibration factor. The offset compensation (see above) is added.

Since the time constant of the cavity is much smaller than the filling time ($\tau_{\mathrm{cav}} = 2.7\,\mu$s, $t_{\mathrm{fill}} = 30\,mu$s), a constant value will be reached within this time. Using only a constant as feedforward table that the incident power is turned on in an extremely short time of below $1\,\mu$s (depending on the output bandwidth of the klystron). If no field is inside the gun cavity nearly the whole incident wave is reflected. So there will be a spike in the reflected power at the beginning of the rf pulse which decays while the field in the cavity increases.

At first this spike has the power of the incident wave. Such a high reflected power can lead to an electrical spark caused by high voltage in the coupler which could damage it. To avoid such sparks the forward power is switched on more slowly following an exponential rise with a time constant τ_{fill} chosen by the operator to minimize the peak of the reflected power. This time constant should be about $10\,\mu$s. Until the end of the filling time ($t = t_{\mathrm{fill}}$) of the cavity (normally $t_{\mathrm{fill}} = 30\,\mu$s) the feedforward table follows the formula

$$FF(t) = \frac{1 - \exp(-\frac{t}{\tau_{\mathrm{fill}}})}{1 - \exp(-\frac{t_{\mathrm{fill}}}{\tau_{\mathrm{fill}}})}. \tag{5.5}$$

During the flat top time the currently used feedforward table is constant and after that it is zero. The phase is set by rotating this table in the complex plane (i.e., multiplying with $e^{i\phi}$). After this the calibration and offset compensation is done.

The phase change due to the change in the tuning of the cavity during the pulse could be compensated, but this requires a precise knowledge of the detuning during the pulse. This is quite difficult to measure (see section 5.4.3). An algorithm for an adaptive feedforward to compensate this phase change and repetitive errors of the klystron with an optimized feedforward table has been developed during the last months. It will be tested on the gun in the next few weeks.

5.4.6 Feedback Control

To reach the required field stability a feedback system is needed in addition to the feedforward. Until now only the forward power was controlled. The goal was to test the feedback and to stabilize the power from the klystron. In the future the cavity will be included into the feedback loop. To do this the field inside the cavity is calculated as the sum of the incident and the reflected wave after the field detectors are calibrated correctly as described above. This has to be implemented in the DSP code. The control algorithm stays the same. The calculation steps done in the DSP are described in this section.

Applying Digital Lowpass Filter

The envelope of the incident field is converted to I and Q signals by the AD8347 detector (see 5.2.1). This signals are sampled by an ADC with 1 MHz sampling frequency. When the signal are sampled it is multiplied with the calibration factor.

After this a digital lowpass filter can be applied to the signal. The sampling changes the continuous time t into time steps $z = t/\Delta t$, where the time Δt is the time between two sampling points, so for a sampling frequency of 1 MHz it is $\Delta t = 1\,\mu$s. The filtered signal is calculated by the formula:

$$\overline{V}_{\mathrm{z}} = \frac{1}{N} V_{\mathrm{z}} + (1 - \frac{1}{N}) \overline{V}_{\mathrm{z\text{-}1}} \tag{5.6}$$

V_{z} is the measured field at the time step z, $\overline{V}_{\mathrm{z}}$ is the filtered signal at the time z, and N is a parameter of the filter which changes the cutoff frequency of the lowpass. With $N = 1$ the filter is turned off, the higher the N, the lower the cutoff frequency of the filter. The filter is used to get rid of a bit of the detector noise. An other advantage especially for the feedback on the klystron is that the gain of the loop is lower for higher frequencies. This makes it possible to increase the gain (see chapter 4.1). If the N in the

lowpass is too high, the time the feedback needs to compensate errors gets too long. Tests have shown that a good choice is $N = 2$.

Calculating Error Signal

After the measured signals is filtered, it is subtracted from the setpoint table to get the error signal of the field. The setpoint table is a table that consists of the desired field values (I and Q) for every time the output of the field detectors is sampled. During filling time it is assumed that the field follows an exponential curve from zero to a saturation higher than the desired value for the flat top. The level of the flat top should be reached after the filling time. The duration of the filling time t_{fill}, the calibration (C_{cal}) that converts the numbers in the DSP to the gradient in the gun, and the desired gradient (E_{acc}) are given by the user. The setpoint at the time t during filling time is:

$$SP(t) = E_{\text{acc}} C_{\text{cal}} \frac{1 - e^{-\frac{t}{\tau_{\text{SP}}}}}{1 - e^{-\frac{t_{\text{SP}}}{\tau_{\text{SP}}}}} \tag{5.7}$$

The time constant τ_{SP} is adjusted so that the setpoint curve follows the field inside the cavity as well as possible, otherwise oscillations will occur when the feedback is turned on. If the control loop only includes the incident wave the time constant of the setpoint curve is the same as that of the incident wave ($\tau_{\text{SP}} = \tau_{\text{fill}} \approx 10\,\mu\text{s}$, see chapter 5.4.5). If the reflected wave is included this time constant is the sum of the time constant of the filling time and that of the cavity ($\tau_{\text{SP}} = \tau_{\text{fill}} + \tau_{\text{cav}} \approx 13\,\mu\text{s}$).

The flat top should be as constant as possible, so the setpoint is just $E_{\text{acc}} C_{\text{cal}}$ for every time step. Since the digital lowpass is applied to the measured field values, it has to be applied in the same way to the setpoint. (One could also apply the filter to the error signal after the measured values are subtracted from the setpoints, but since the filtering is a linear operation it makes no difference.)

PI Control

The error signal is then used for the PI control. How a PI control works is discussed in chapter 4.1. In the DSP everything is discrete in time since the signals are sampled with a constant rate. A time discrete integration means that the value from the last timestep is added to the newest measured error signal.

The parameters for the PI control are the gains of the proportional and the integrational part. To have the opportunity to turn them on and off, this parameters are in tables, like the setpoint and the feedforward, with values for every timestep. Experiments have shown that the integrator is not stable if it is turned on during filling time, so we chose the integrator gain to be 0 during filling time.

When the output of the PI controller is calculated it is added to the next value of the feedforward table. This sum is converted to an analog signal and sent to the vector modulator which controls the incident wave. The whole scheme is represented in figure 5.24.

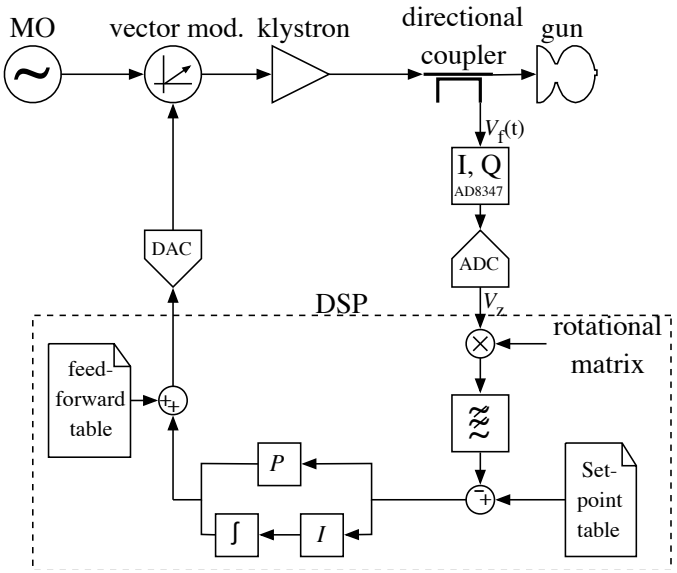

Figure 5.24: Schematics of the close loop control on the klystron

During the current run of the VUV-FEL accelerator we want to control the field in the gun cavity. To do this we have to use forward and reflected power. After the measurement of the two fields both are sampled with 1 MHz. To be able to make a correct control on forward and reflected power, it is important to know the difference in phase and amplitude between the forward power from the klystron and the reflected power from the gun at the coupler. Since we don't measure directly at the coupler, we have to find two matrices, that compensate the phase shifts and attenuation of the incident and the reflected wave until they reach the detectors.

5.4.7 Adaptive Feedforward

The adaptive feedforward is based on the inversion of the transfer function of the cavity (see chapter 4.2).

To reduce the statistical noise the incident and the reflected field of several rf pulses is measured and the average is taken. Than the field in the gun cavity is reconstructed by summing up the averaged incident and reflected waves. With the reconstructed cavity field and the setpoint curve the error signal for each point of the rf pulse is calculated as in the case of the feedback (see above). For further noise reduction an averaging filter is used.

To this filtered error signal a digital filter with the inverse transfer function of the gun cavity applied. To get the new feedforward table a fraction (70 % - 90 %) of the result of this is added to the old feedforward table. Simulations with the parameters of the superconducting cavities suggest that the adaptive feedforward is improved by adding a fraction of the correction of feedback to the new feedforward table. If this is true for the gun will be tested soon.

5.5 Generation of the Incident Wave

The field in the cavity is controlled by changing the incident wave with a vector modulator (AD8346). This vector modulator is the counterpart of the IQ detector (AD8347). Two signals representing real and imaginary part of a wave are sent to the modulator and an incident wave coming from the master oscillator will be modulated in a way that the amplitude of the output is proportional to the absolute value of the complex input[2] and shifted in phase by the angle of the complex input compared to a reference wave from the master oscillator. This modulated signal is amplified by a preamplifier and afterwards by a the klystron.

The amplitude of the output should be independent of the phase of the control signal. This was checked in the accelerator. A phase sweep has been done and the amplitude of the incident power was measured. The result of this measurement is shown in figure 5.25. The amplitude is obviously not independent of the phase. The source of this error is currently investigated. It can be caused by the vector modulator itself, but it is more probable that the source is are DACs which may convert positive and negative values differently.

[2]With complex input I mean the two inputs I and Q seen as one complex number $Z = I + i \cdot Q$.

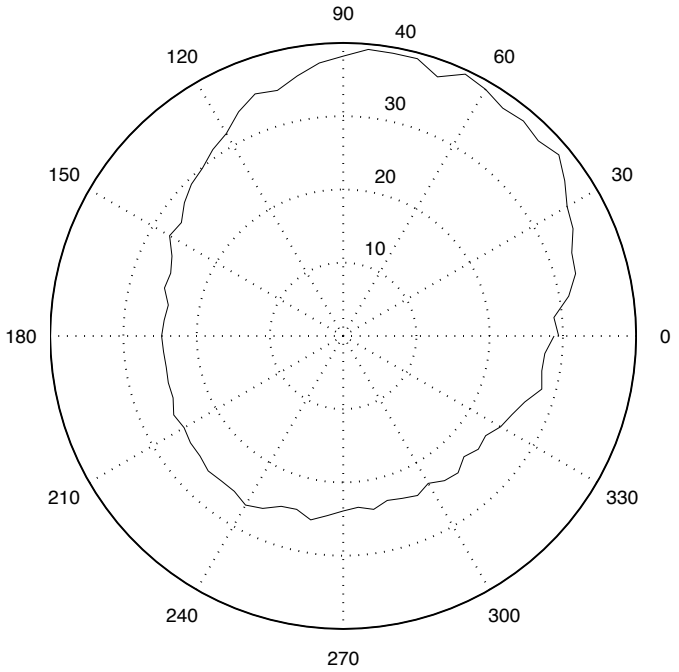

Figure 5.25: Amplitude of the incident wave as a function of the phase (The picture is taken from the electronic logbook of the VUV-FEL [16])

Chapter 6

Results

Between February 2004 and June 2004 the first data concerning performance of the injector of the new VUV-FEL accelerator have been taken. As said in the previous chapter the feedback system for the gun was only used to stabilize the incident wave and not the sum of the incident and the reflected wave, since the DSP code was not finished.

In this chapter the achieved field stability is investigated and the performance of the feedback is described. This is compared to the requirements.

6.1 Field Stability Without Feedback

Changes of the field inside the cavity during one rf pulse are caused by changes of the incident wave and by the variation of the tuning of the gun resonator.

During one pulse of 200 μs duration the forward power changes in amplitude by about 2 %. The phase changes under the same conditions by 10°. The phase change is strong at the beginning of the pulse. During the flat top time where the field stability is important the phase change is less the longer the pulse is (see figure 6.1). During the last 160 μs of the 200 μs long pulse the amplitude change is only 1 %. If averaged over many pulses, a 250 kHz ripple on the signals of the IQ detector can be seen which is stable in phase compared to the sampling points of the ADC reading the detectors. This ripple is some kind of crosstalk from the downconverters. How the 250 kHz signal from the downconverter reaches the IQ detector is not yet known; presumably it is transmitted via the ground. With 0.2° in phase this ripple is below the detector noise and also below the requirements of the field stability. Thus a suppression it is not important to reach the requirements, but it limits the precision of the calibration of the reflected power (see chapter 5.4.2).

For relatively long microwave pulses (600 μs) with high power (3.5 MW forward power) the phase of the reflected wave changed between the begin-

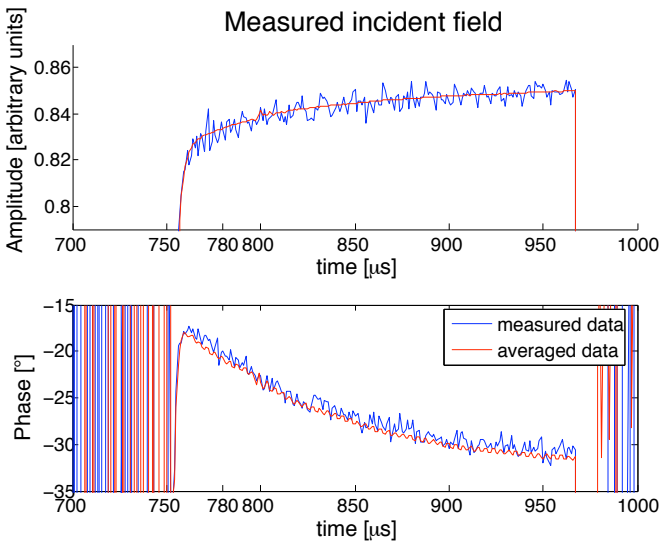

Figure 6.1: Shape of the incident wave during a 200 μs long pulse (single pulse and average over 1200 pulses

ning of the RF pulse and the end 600 μs later by about 25°. The phase change of the reflected wave during one 200 μs pulse with 3.5 MW forward power can be seen in figure 6.2. Since we have no field probe, we can only assume that this is caused by the detuning of the gun as theory predicts. If this assumption is correct the reflection coefficient $\Gamma = \frac{V_{\text{ref}}}{V_{\text{for}}}$ lies on a circle for every point measured during the pulse, since $\Gamma = \frac{Z_{\text{cav}}-Z_0}{Z_{\text{cav}}+Z_0}$ (equation 3.14) describes a circle in the complex plane if the imaginary part of Z_{cav}, which is the detuning, is changed. During one pulse the change of the tuning of the cavity is not so big that the curvature of the resulting circle can be seen easily. The tuning of the cavity changes by 6 kHz during one pulse with 3.1 MW incident power (see figure 5.23 in chapter 5.4.2). This results in a phase shift of the cavity field compared to the incident wave of 5°. Thus it is difficult to see if the measured points of the reflected wave lie on a circle. By detuning the gun extremely we have been able to see this, though. This supports the assumption at least for very big detuning in the order of the bandwidth (about 60 kHz).

The amplitude change of the field inside the cavity is composed of the change of the incident wave and the change due to the variation in the tuning of the gun cavity. The tuning of the gun cavity changes by up to 10 kHz for long pulses (800 μs) and high incident power (3.2 MW) (see 5.4.3). The resulting phase change is 9.5°, the amplitude change 1.4 %.

Without feedback and adaptive feedforward the total field instabilities during one pulse are about 3 % in amplitude and up to 15° in phase. Cor-

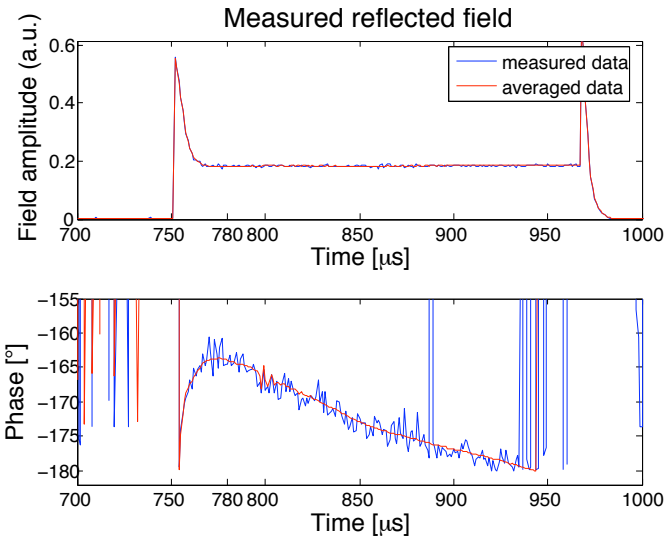

Figure 6.2: Shape of the reflected wave during a 200 μs long pulse (single pulse and average over 1200 pulses

rection with the feedback only is not possible (see below), but comparison of many successive pulses show that the field changes described above are repetitive, i.e., the shape is nearly the same every pulse. This means it is possible to compensate them with an adaptive feedforward.

Non repetitive errors are changes in the tuning of the gun between the pulses, fluctuations of the klystron power and noise. The statistical noise of the detector signals has an amplitude of 0.75 $\%_{\mathrm{rms}}$ in amplitude and $0.5^{\circ}_{\mathrm{rms}}$ in phase. The amplitude and phase change of the incident wave between the pulses is about 0.1 $\%_{\mathrm{rms}}$ and $0.3^{\circ}_{\mathrm{rms}}$ and so below the noise levels and the requirements.

After turning on the gun it takes at least 30 min until the control system has stabilised the temperature. The precision of the control is ± 0.01°C (see figure 6.3), the frequency is stabilised to ± 200 Hz which causes 0.5° phase shift peak to peak. This is verified experimentally. The non repetitive errors sum up to nearly 1 % amplitude and 1° in phase. This is near to the requirements even for the XFEL so that no high proportional gain (more than 4) in a feedback loop is needed to reach the requirements if the repetitive errors can be compensated by the feedforward.

6.2 Feedback Performance

Until the DSP code includes the reflected wave the feedback is only used to stabilize the incident wave as described above (chapter 5.4.6). As one

Figure 6.3: Temperature of the gun (near iris) after interlock. The pulse length was increased slowly to 600 μs at a power of 3 MW. Then the temperature was left to stabilise.

would expect from theory (chapter 4.1) the possible feedback gain is small ($G_{\mathrm{P}} \approx 2$) if the cavity is not included into the feedback loop.

Figure 6.4 shows the performance of the feedback with different loop gains. You can see the error suppression with low gain compared to the case without feedback. With too high gain the feedback gets unstable and oscillations occur[1].

The deviation from the setpoint is reduced by the feedback with gain G_{p} by a factor of $\frac{1}{1+G_{\mathrm{P}}}$. With a gain of two the error is reduced to $\frac{1}{3}$. To correct the statistical errors which remain even with an optimal feedforward algorithm, the gain has to be increased to a least 4 if the requirements are to be reached. This should be possible if the reflected wave is included in the feedback loop and the calibrations are done properly.

[1]The gain factors given in the legend of the picture may not be calibrated correctly. The real values might differ by 50 %.

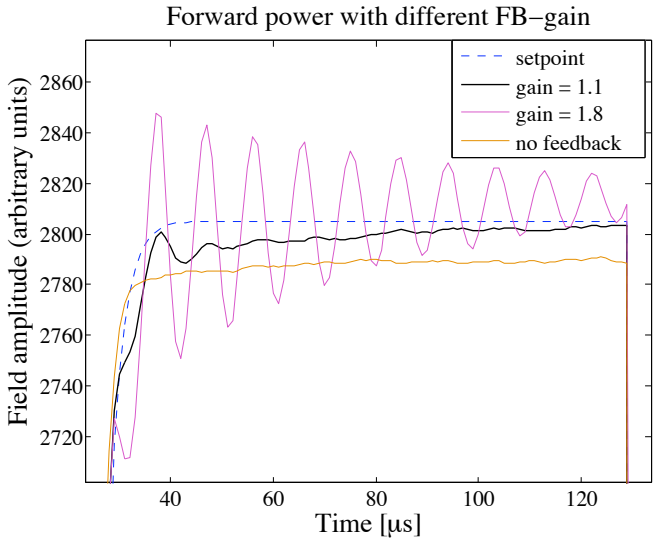

Figure 6.4: Forward power and setpoint with varying feedback gain

Chapter 7

Conclusion and Outlook

7.1 Counclusion

The field detectors we use have a sufficiently low noise level to reach the requirements for the field stability, though a larger safety margin would be preferable.

The performance of the feedback is as expected by the theory. If it stays this way the gain will be higher if the reflected wave and thus the cavity is included in the feedback. This implementation will be made within the next few month. The increased possible gain should then be high enough to control the non repetitive errors. To reach the requirements the repetitive errors have to be reduced independent of the feedback.

To achieve the required field stability the adaptive feedforward has to be implemented.

If the adaptive feedforward and the feedback will perform as expected the field stability given by the requirements ($\pm 0,5\,\%$ Amplituden, $\pm 2^\circ$ phase) can be reached.

The most sever difficulty is the calibration of the reflected wave relative to the incident wave. Until now the precision of the reconstructed cavity field presumably is $0.5\,\%$. This is valid if the calibration of the reflected wave relative to the forward power is working as hoped and if it is stable. This will be difficult to confirm without a probe by looking at the beam only. In my opinion it should be reconsidered if the loss in field symmetry caused by a probe really is worse than the problems caused for the control of the field.

7.2 Future Imrovements

Until now the reflected power is not implemented in the control loop. This is expected to be done in one or two months (until December 2004 or January 2005). Then we will see if the control will provide a field as stable

as expected. To be more secure that the requirements can be fulfilled and for stronger requirements in future accelerators (for example the european X-FEL) improvements in the used hardware are now planned or developed. Some of these improvements are shortly described in the next section.

For better operability and stability some extensions to the existing software could be made. The second section of this chapter contains some proposals.

Improvemenst of the Hardware

With hardware improvements the field detection and the control system might become better.

The detectors can be improved by using faster ADCs. The higher sampling rate can give us the opportunity to average over many samples and thus reduce the noise. With a high sampling rate of the ADCs the downconverters (see 5.2.5) can become very useful for the gun control. Compared to the other detectors they have the advantage that DC offsets cause no problems. Currently the building of downconverters with an intermediate frequency of 81 MHz, instead of the 1 MHz we use now, is planned.

The control system might be improved by the use of an FPGA[1] based control system replacing or supplementing the DSP system. FPGAs provide the possibility of extremely fast calculations. To use this technology decreases the delay time in the control loop from now about $4\,\mu$s by up to $2\,\mu$s, especially when combined with high speed ADCs. Thus a higher feedback gain will be made possible. The remaining time delay is mostly due to the cables and the klystron. An FPGA based control system is currently developed for the VUV-FEL and for X-FEL.

Extensions of the Software

It takes nearly half an hour for the temperature control to stabilise the temperature at the setpoint. Partly because the temperature control is based on heating and cooling through the water flow which changes the temperature only within minutes. The temperature control is made more difficult and tends to oscillations because the heating and cooling of the cavity changes the tuning of the cavity and the higher the detuning of the cavity the less power is dissipated in the cavity walls at a constant incident power. This mechanism makes the temperature regulation difficult and increases the time needed to stabilise the tuning.

To increase the speed especially after the gun has cooled down the resonance frequency of the gun could be measured and the incident wave can be modulated to match those frequency. While the gun is heated the frequency

[1] FPGA - Field programmable gate array

of the driving power can track that of the gun resonator until the desired frequency is reached.

The frequency of the gun can be measured with a test pulse that sweeps through a frequency range. This way a resonance curve of the gun can be taken and the resonance of the gun can be found. Such a resonance curve has been taken (see figure 7.1).

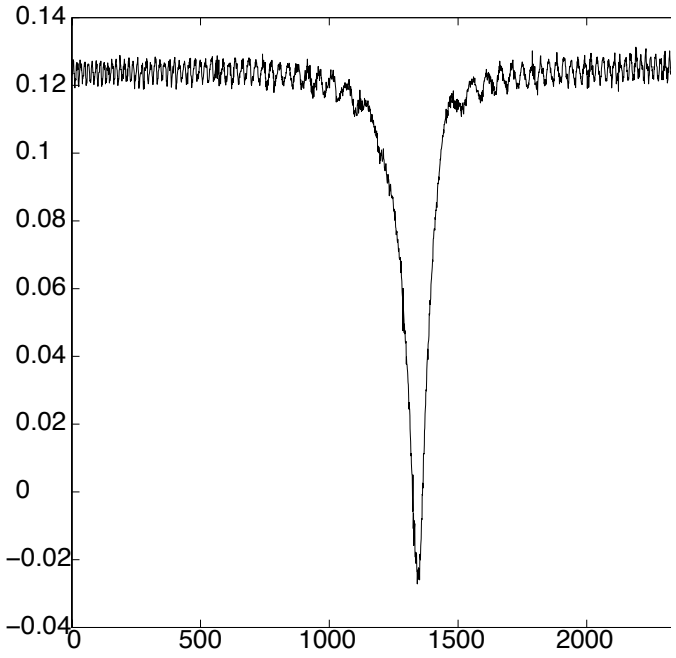

Figure 7.1: Resonance curve of the gun. The logarithm of the reflected power is plotted against the time during the frequency sweep on the horizontal axis.

The modulated frequency can be generated using the vector modulator and shifting the incident wave by some degrees in phase every time the DAC gives a new value. For example to shift the incident wave by 250 kHz the phase shift between the DAC outputs has to be 90° at a clock frequency of the DAC of 1 MHz. Of cause the resulting wave is not really a wave with the changed frequency, but it has a Fourier component with the shifted frequency which will excite the cavity.

The control itself might be improved by the use data from the electron beam. Since we have no probe the beam is the most direct method to get information about the field it has interacted with when it went through the cavity. The different possibilities have not been investigated closely, yet. This is an interesting work to be done in the future.

Appendix A

Derivation of the Equation for Envelope of the Field

The gradient of the electric field in the cavity can be described by the equation 3.9:

$$\ddot{V}(t) + \frac{\omega_0}{Q_\mathrm{L}}\dot{V}(t) + \omega_0^2 V(t) = \frac{\omega_0 R}{Q_\mathrm{L}}\dot{I}(t)$$

Let us assume we have a harmonic current from the klystron. Then we can divide the voltage and the current into the fast harmonic oscillation with the frequency ω and a slowly alternating amplitude $V_0(t)$:

$$\begin{aligned} V(t) &= V_0(t)e^{i\omega t} \\ \Rightarrow \dot{V}(t) &= \dot{V}_0(t)e^{i\omega t} + i\omega V_0(t)e^{i\omega t} \\ \Rightarrow \ddot{V}(t) &= \ddot{V}_0(t)e^{i\omega t} + 2i\omega\dot{V}_0(t)e^{i\omega t} - V_0(t)\omega_0^2 e^{i\omega t} \end{aligned} \tag{A.1}$$

$$\begin{aligned} I(t) &= I_0(t)e^{i\omega t} \\ \Rightarrow \dot{I}(t) &= \dot{I}_0(t)e^{i\omega t} + i\omega I_0(t)e^{i\omega t} \end{aligned} \tag{A.2}$$

If we plug A.1 and A.2 into 3.9, we get:

$$\begin{aligned} \ddot{V}_0(t) + 2i\omega\dot{V}_0(t) - V_0(t)\omega^2 + \frac{\omega_0}{Q_\mathrm{L}}\dot{V}_0(t) + \frac{i\omega\omega_0}{Q_\mathrm{L}}V_0(t) + \omega_0^2 V_0(t) \\ = \frac{\omega_0 R}{Q_\mathrm{L}}\dot{I}_0(t) + \frac{i\omega\omega_0 R}{Q_\mathrm{L}}I_0(t) \end{aligned}$$

Using $\frac{\omega_0}{Q_\mathrm{L}} = 2\omega_{1/2}$ (equation 3.26) we get:

$$\ddot{V}_0(t) + \Big(2\omega_{1/2} + 2i\omega\Big)\dot{V}_0(t) \; + \; \Big(\omega_0^2 - \omega^2 + 2i\omega\omega_{1/2}\Big)V_0(t) \\ = 2\omega_{1/2}R\Big(\dot{I}_0(t) + i\omega I_0(t)\Big)$$

After multiplying both sides with $-\frac{i}{2\omega_{1/2}}$ we have:

$$-\frac{i}{2\omega_{1/2}}\ddot{V}_0(t) + \Big(1 - \frac{i\omega_{1/2}}{\omega}\Big)\dot{V}_0(t) \; - \; \Big(i\frac{\omega_0^2 - \omega^2}{2\omega} - \omega_{1/2}\Big)V_0(t) \\ = \omega_{1/2}R_\mathrm{L}\Big(I_0(t) - \frac{i}{2\omega_{1/2}}\dot{I}_0(t)\Big)$$

To make this a bit easier to handle we have to use approximations. The changes of the input from the klystron $I_0(t)$ are relatively slow compared to the harmonic frequency ω, so we can assume that $\frac{\dot{I}_0(t)}{2\omega} \ll I_0(t)$. The field in the cavity changes even slower due to the relatively high quality of the cavity. Thus we can also assume that $\frac{\ddot{V}_0(t)}{2\omega} \ll \dot{V}_0(t)$. So we can neglect the terms with $\dot{I}_0(t)$ and $\ddot{V}_0(t)$.

$$\Big(1 - \frac{i\omega_{1/2}}{\omega}\Big)\dot{V}_0(t) = \Big(i\frac{\omega_0^2 - \omega^2}{2\omega} - \omega_{1/2}\Big)V_0(t) + \omega_{1/2}RI_0(t)$$

With $(\Delta\omega) := \omega - \omega_0$ we finally come to:

$$\dot{V}_0(t) = \frac{\omega}{\omega - i\omega_{1/2}}\Big[\Big(i\frac{(\Delta\omega)^2}{2\omega} - i(\Delta\omega) - \omega_{1/2}\Big)V_0(t) + \omega_{1/2}RI_0(t)\Big] \qquad \text{(A.3)}$$

To make this equation even more handy, we can also assume that the detuning of the cavity and the bandwidth of the cavity are small compared to the driving frequency ($\Delta\omega \ll \omega$ and $\omega_{1/2} \ll \omega$). In this case equation A.3 becomes:

$$\dot{V}_0(t) = \Big(-i(\Delta\omega) - \omega_{1/2}\Big)V_0(t) + \omega_{1/2}RI_0(t) \qquad \text{(A.4)}$$

Appendix B

Schematic of the Gun Detector Box

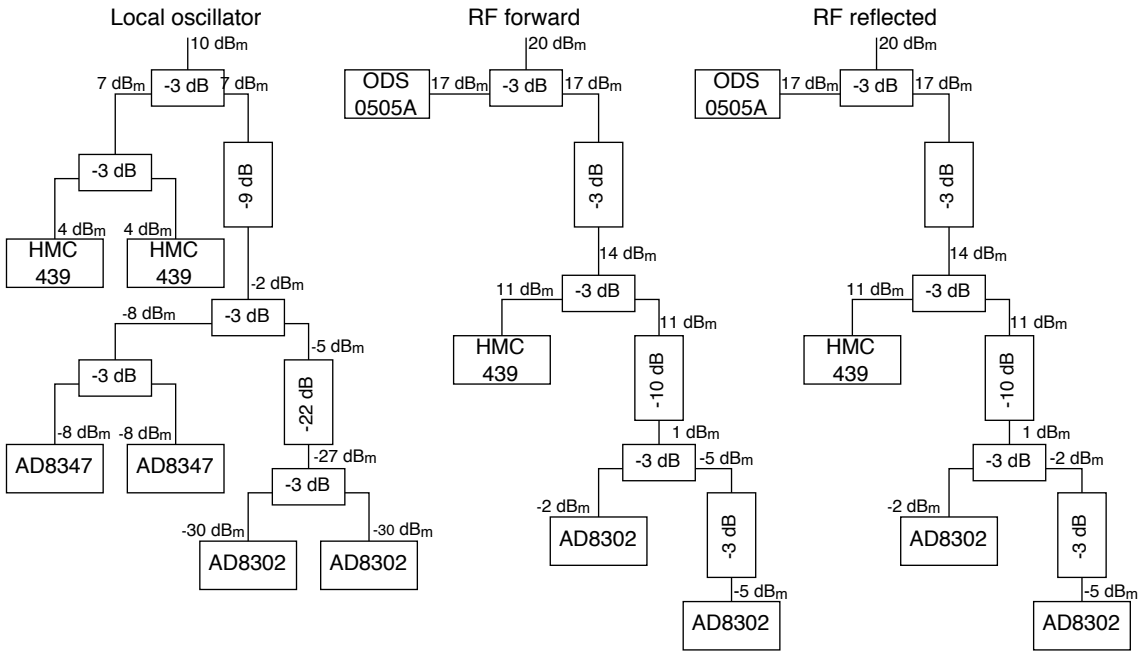

Figure B.1: Schematic of the power distribution inside the RF Gun detector box.

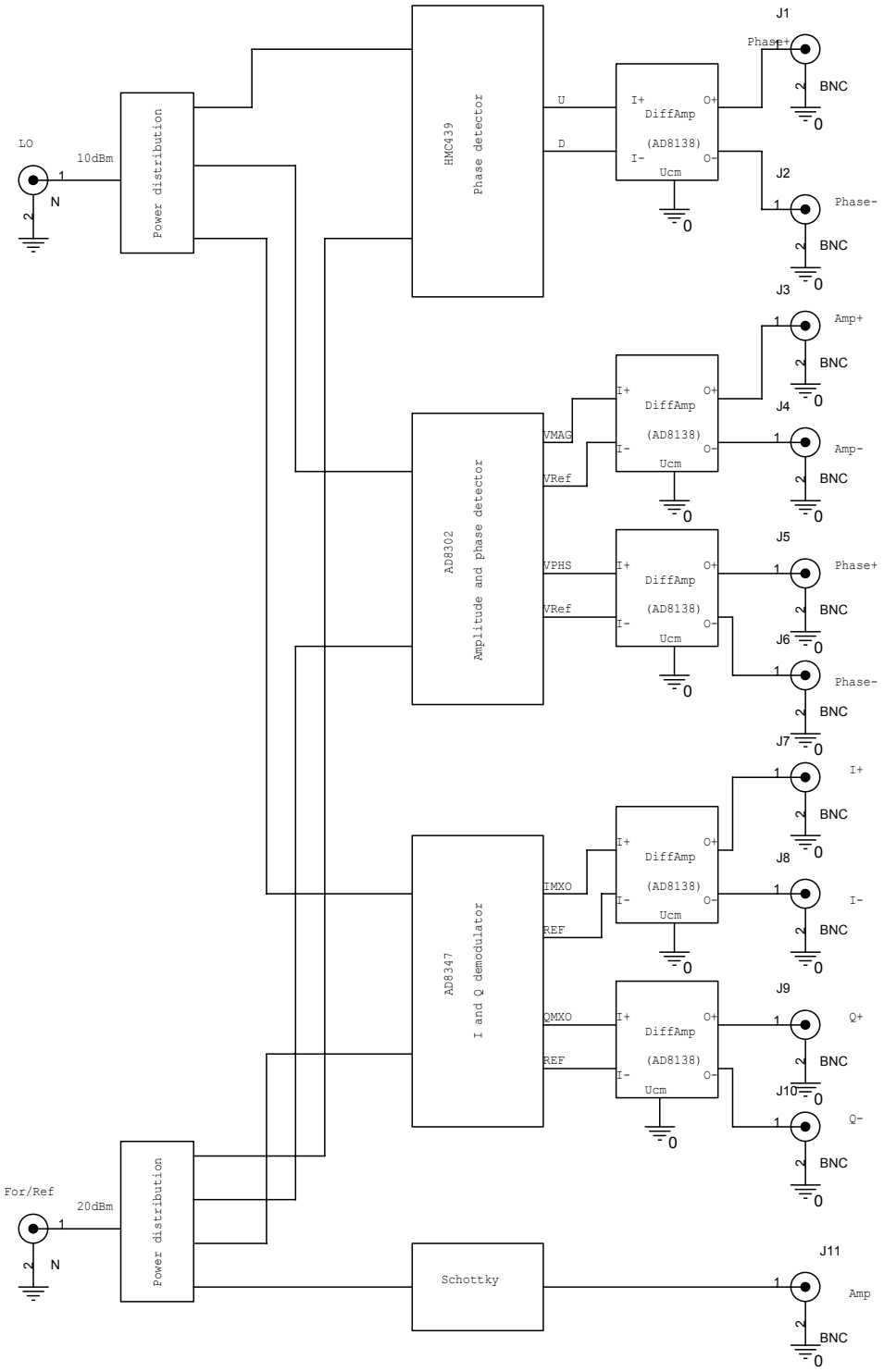

Figure B.2: Block scheme of the gun detector box. The scheme only illustrates the setup for one input signal. The box contains the same for the forward and the reflected wave.

Appendix C

Circuit Diagrams

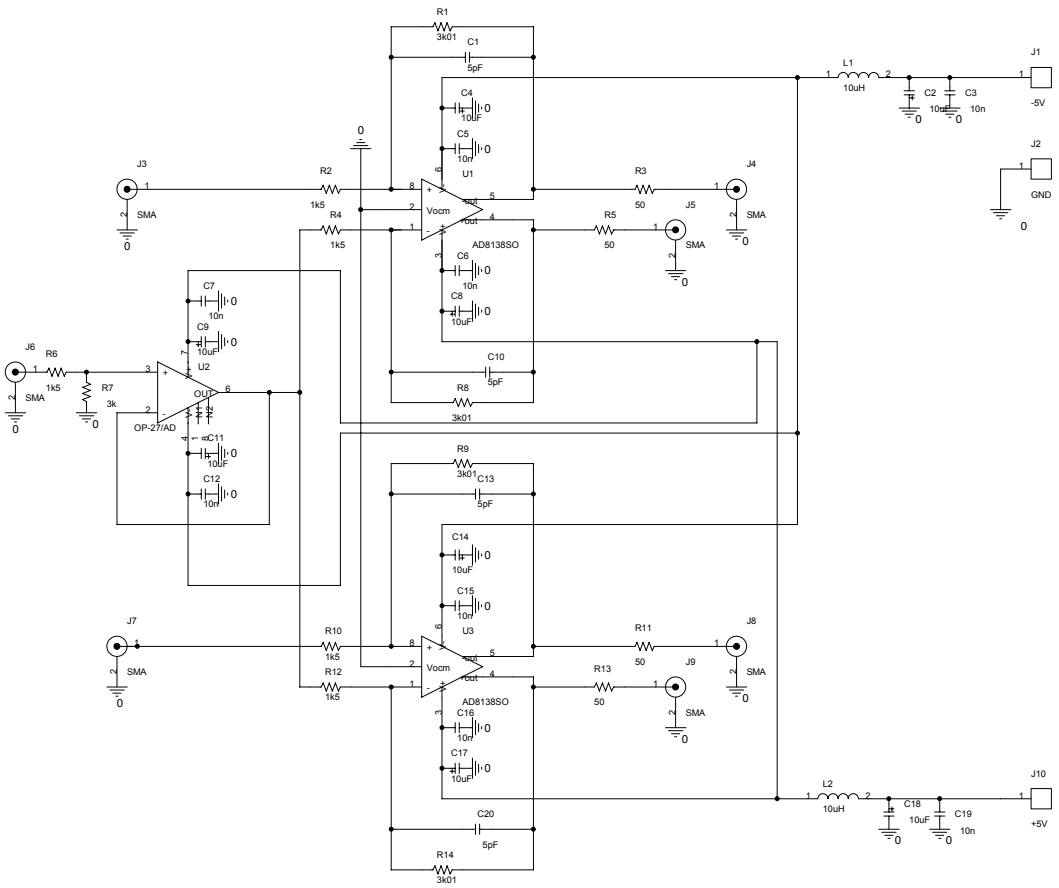

Figure C.1: Circuit diagram of the output amplifier for the AD8302

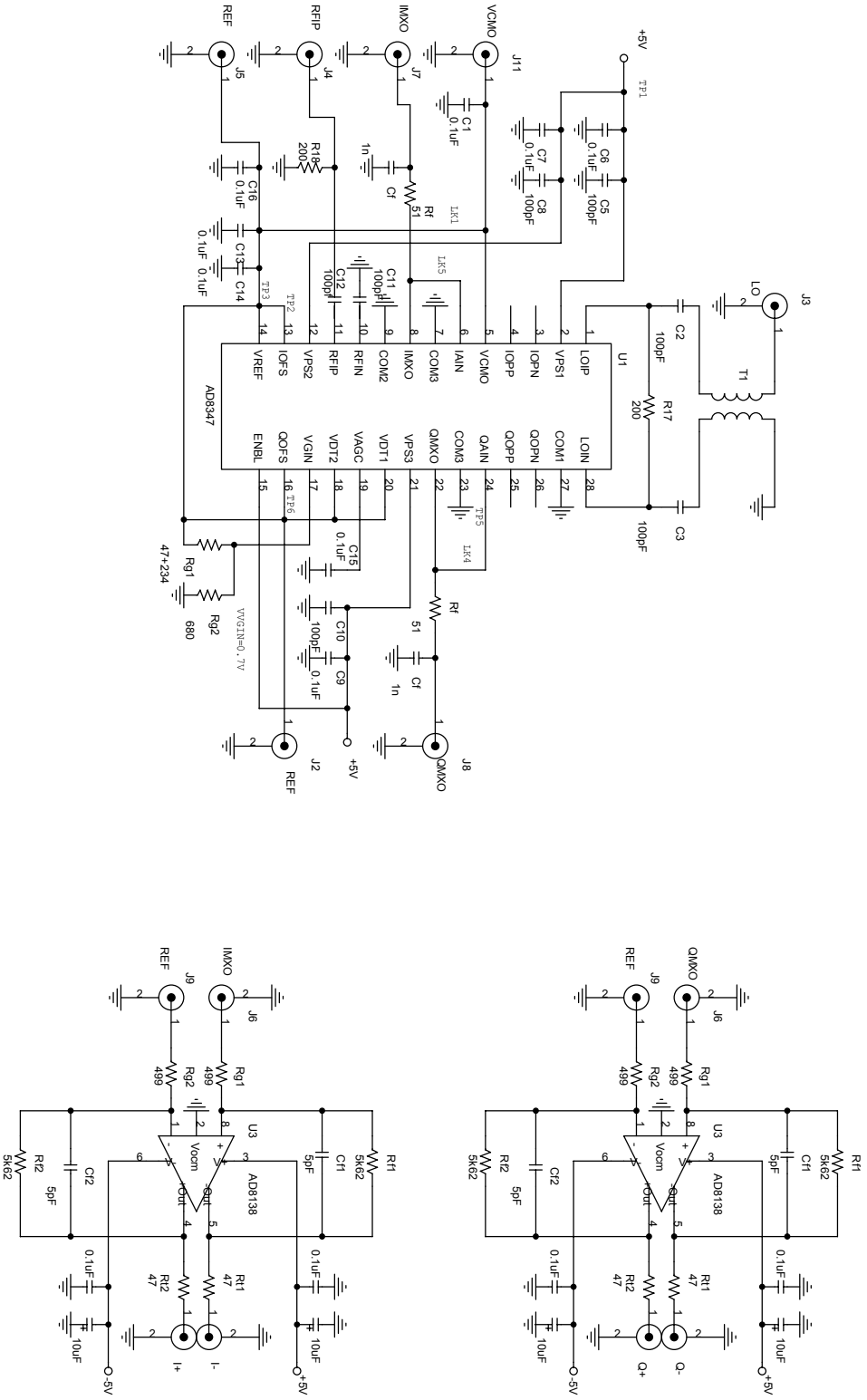

Figure C.2: Circuit diagram of the modified evaluation board for the AD8347 and the output amplifiers used with this detectors

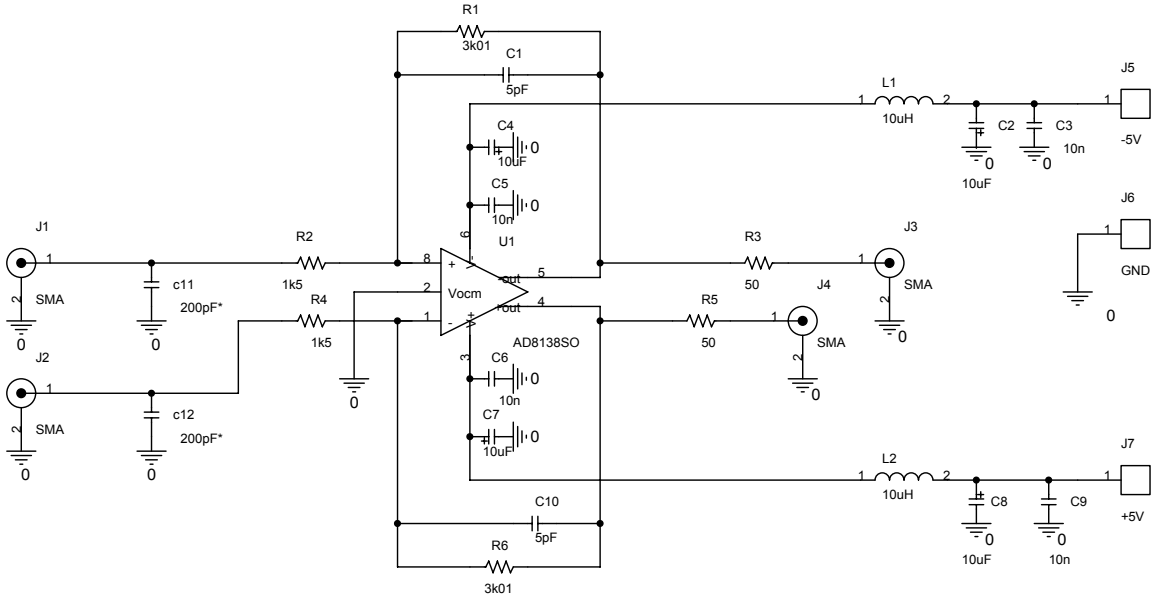

Figure C.3: Circuit diagram of the output amplifiers for the HMC439 detectors

Bibliography

[1] A. S. Gilmour. *Principles of Traveling Wave Tubes*. Artech House, Inc., 1994.

[2] Analog Devices. *AD8302 - RF/IF Gain and Phase Detector*. Datasheet from Analog Devices.

[3] Analog Devices. *AD8347 - Direct Conversion Quadrature Demodulator*. Datasheet from Analog Devices.

[4] D. M. Pozar. *Microwave Engineering*. John Wiley & Sons, Inc., 2nd edition, 1998.

[5] DESY - Deutsches Elektronen-Synchrotron. TESLA - The Superconducting Electron-Positron Linear Collider with an Integrated X-Ray Laser Laboratory. Technical report, TESLA - Collaboration, March 2001.

[6] DESY - Deutsches Elektronen-Synchrotron. *Was ist XFEL?* World Wide Web, http://www.desy.de/pr-info/desyhome/html/presse/hginfos/xfel/was.html, 2004.

[7] G. Ludyk. *Theoretische Regelungstechnik*, volume 1. Springer-Verlag, 1995.

[8] G. von Walter. Entwicklung und Optimierung einer Regelung für die Hochfrequenz-Photoelektronenquelle am TTF-Linearbeschleuniger. Master's thesis, RWTH Aachen, Dezember 1999.

[9] Hittite. *HMC439QS16G - HBT Digital Phase-Frequency Detector, 10-1300 MHz*. Datasheet from Hittite.

[10] J. Baehr et al. Behavior of the TTF2 RF Gun with long pulses and high repetition rates. In *TESLA Note 2003-33*, 2003.

[11] J. Feldhaus, D. Nölle. Beam Diagnostics at the VUV-FEL Facility. In *Proceedings of the EPAC 2004, Lucerne*, 2004.

[12] J. Feldhaus, J. Roßbach, H. Weise. Freie-Elektron-Laser. *Spektrum der Wissenschaft*, Dossier 2/1998:106–111, February 1998.

[13] M. Ferrario, K. Flöttmann, B. Grigoryan, T. Limberg, Ph. Poit. Conceptual Design of the XFEL Photoinjector. Technical Report XFEL-notes 2001-03, TESLA-Collaboration, February 2001.

[14] T. Schilcher. *Vector Sum Control of Pulsed Accelerating Fields in Lorentz Force Detuned Superconducting Cavities*. PhD thesis, Universität Hamburg, 1998.

[15] The TESLA Test Facility FEL team. SASE FEL at the TESLA Facility, Phase 2. Technical Report TESLA-FEL 2002-01, DESY, June 2002.

[16] TTFelog - Electronic Logbook for TTF2, 07.09.2004.

[17] W. Demtröder. *Experimentalphysik - Elektrizität und Optik*, volume 2. Springer-Verlag, 1995.

[18] Yujong Kim et al. S2E Simulations on Jitter for European XFEL Project. In *LINAC 2004, Lübeck, Germany*, 2004.

Acknowledgements

I am grateful for the opportunity to participate at the work on the VUV-FEL. It was a very inspiring interesting and instructive time.

I thank Alexander Brandt, Bastian Lorbeer, Henning Weddig, Matthias Hoffman, Nicolai Ignachin and Valeri Ayvazyan for supporting my work with many helpful discussions and information.
I owe sincere thanks to Stefan Simrock for his numerous ideas, hints and explanations.
Especially, I thank my supervising Professor Peter Schmüser for helping me in completing this thesis.
I want to express my gratitude for the stimulating and friendly work environment to all members of the TTF team, especially the members of the FLA and the LLRF group.
Finally, I thank Annette for the words 'has been'.

Erklärung

Hiermit versichere ich, die Arbeit sebständig und nur unter Verwendung der angegebenen Quellen und Hilfsmittel verfasst zu haben. Ich gestatte die Veröffentlichung dieser Arbeit.